MACHINING OF COMPOSITES—A NEW APPROACH
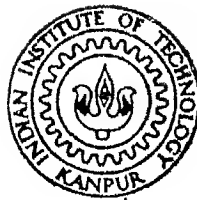
by

SANJIV TANDON

DEPARTMENT OF MECHANICAL ENGINEERING

INDIAN INSTITUTE OF TECHNOLOGY, KANPUR

JULY, 1987

MACHINING OF COMPOSITES — A NEW APPROACH

A Thesis Submitted
In Partial Fulfilment of the Requirements
for the Degree of

MASTER OF TECHNOLOGY

by

SANJIV TANDON

to the

DEPARTMENT OF MECHANICAL ENGINEERING

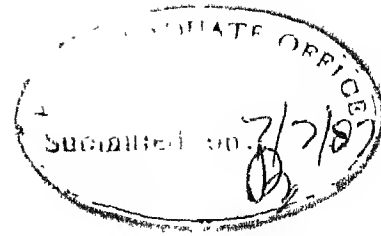INDIAN INSTITUTE OF TECHNOLOGY, KANPUR

JULY, 1987

CERTIFICATE

This is to certify that the thesis entitled,

"MACHINING OF COMPOSITES : A NEW APPROACH" by Sanjiv Tandon

is a record of the work carried out under our supervision

and has not been submitted elsewhere for a degree.

(V.K. Jain)
Assistant Professor
Mechanical Engineering Dept.
Indian Institute of Technology
Kanpur-208016

(P. Kumar)
Professor
Mechanical Engineering Department
Indian Institute of Technology
Kanpur 208016

6 July, 1987.

ACKNOWLEDGEMENTS

I wish to express my deep sense of gratitude and appreciation to thesis advisors Dr. V.K. Jain and Dr. P. Kumar, for their valuable guidance throughout the present work. I greatly value their friendly advices, constant encouragement and above all their humility.

I am obliged to Dr. B.D. Aggarwal for the various fruitful discussions that I had with him during the course of present work. I am also indebted to Dr. S.C. Korea for his generous attitude in helping me with the instrumentation for the apparatus.

Ranjit Singh (Ph.D., Chemistry) and K.K. Bajpai must be thanked for going out of their ways to help me with the experimentation and Asit Nema (M.Tech.,Civil) for assisting me in the computer work. I acknowledge Girish Thakkar's (M.Tech., Mechanical) aid in the plotting of graphs and for proof reading of the text.

Rajesh Aggarwal and S. Gupta are to be thanked for the valuable assistance rendered throughout this work. I must also thank Messrs Swaran Singh, P.N. Pandey and B.D. Pandey for their full hearted cooperation throughout the present work.

Shri B.K. Jain (ACMS) and Shri Qasim Hussain (ACES) are responsible for the neat tracings of the figures and Shri U.S. Mishra for giving the thesis its present form.

Finally, I need hardly mention the company of my close friends in the institute and the hall of residence which made my stay in IIT Kanpur a memorable experience.

July, 1987.   —Sanjiv Tandon

CONTENTS

LIST OF TABLES

LIST OF FIGURES

LIST OF PHOTOGRAPHS

NOMENCLATURE

A	area of composite laminate (m^2)
d_f	density of fibre (kg/m^3)
d_{fa}	areal density of fabric/mat (kg/m^2)
d_s	density of specimen (kg/m^3)
d_t	density of tool material (kg/m^3)
k^*	optimum specific conductance (milli-mho/cm)
MRR	material removal rate (mg/min)
MRR^*	optimum material removal rate (mg/min)
N	number of CSM/Kevlar fabric layers in a laminate
O_a	average overcut (mm)
O_d	diametral overcut (mm)
O_t	top overcut (mm)
RTW	relative tool wear (%)
RTW^*	optimum relative tool wear (%)
t	thickness of laminate (m)
TWR	tool wear rate (mg/min)
V^*	optimum voltage (volts)
X_1, X_2, X_3	factors (or controllable variables), voltage, fibre volume fraction, specific conductance, respectively
Y_u	response, Eq. 3

ABSTRACT

Fibre reinforced composites, though relatively new materials, have already become important engineering materials. So far the main emphasis of research has been the development of materials, but nowadays more attention is drawn to the industrial production of products made of composites. In this work a new approach for the machining of composites is discussed.

The effect of voltage, electrolyte conductivity, fibre volume fraction and tool geometry on the technological characteristics during Electrochemical Discharge machining of composites has been studied. Some of the experiments have been carried out according to "design of experiments" concept while others have been conducted using one variable at a time approach. Kevlar-epoxy and glass-epoxy composites have been machined using copper/brass as tool material and NaCl as electrolyte. The responses, i.e., material removal rate, tool wear rate, relative tool wear and overcut produced during experimentation are measured and/or calculated. A part of analysis has been done using Computer Program - CADEAG-1. The effects of different factors on the responses are shown in various graphs. Material removal rate and relative tool wear have been optimised using overcut as a constraint. The effect of sludge, which is produced during machining, on electrolyte conductivity has also been studied.

CHAPTER 1

INTRODUCTION AND LITERATURE SURVEY

1.1 COMPOSITE MATERIALS

A material made by the combination of two or more macroconstituents differing in form and/or material composition and that are essentially insoluble in each other is called a composite material.

Fibre reinforced composites are relatively new materials but they have already become important engineering materials. They are well known for their light weight, high strength, high stiffness and controlled anisotropic properties. Additional advantage that composites offer over the conventional materials include flexibility in design, corrosion resistance, etc. Today, fibre composites have found such diverse applications as space vehicles, aircraft, offshore structures, automobiles, protective armours, containers, corrosion resistance coatings, sporting goods and electronics. The most widely used fibrous composites are glass -, graphite- , Kevlar- , boron- , and alumina- fibre composites. Plastics such as epoxy, polyester, etc. are the commonly used matrix materials.

1.2 MACHINING OF COMPOSITES

So far the main emphasis of research has been the development of materials, but nowadays more attention is

drawn to the industrial production of products made of FRP (fibre reinforced plastics). In aerospace and shipbuilding industries, which are almost classic fields of application, the production of single parts is the common case. But in automotive, machine tool and sporting good industries, where mass production predominates, the necessity of fully automated and economic production methods arises. The substitution of metals by plastics with glass, carbon or aramid fibre reinforcement does not only require change in design philosophy, but also affects both the particular production technique and the complete production cycle.

The machining of FRP differs in many respects from metal working. The material behaviour not only is inhomogeneous, but also dependent on fibre and matrix properties, fibre orientation and the type of weave. Therefore, the machining of FRP requires special demands on the geometry and abrasive resistance of tool material.

For the machining of glass and carbon fibre laminates a conventional tool geometry similar to the one used in metal cutting is usable. Since high abrasion resistance is necessary for these compounds, HSS (high speed steel) is unsuitable as a tool material. In order to achieve a high tool life in routing operations, routers with multiple cutting edges like the so-called "diamond cut" are employed. The use of electroplated diamond cutters is also a common practice [1].

In aramid fibre reinforced plastics (AFRP) standard
tools are not applicable without severe material damage
like delamination or fuzzing (as shown in photograph No.1).
Aramid fibres require very keen cutting edges and a tool
geometry which inhibits the fibre displacement in front of
the cutting edge. HSS tools usually achieve insufficient
tool life even in AFRP. In general the tool life may be
increased by coating HSS or carbide with TiN [1]. In some
cases, however, the increase of cutting edge radius due to
coating may result in a complete failure of tool performance.
Moreover, grinding tools which usually possess a negative
rake angle are not suitable for the machining of AFRP. Even
more difficulties are encountered when the composite material
consists of aramid fibres in addition to glass or carbon
fibres, because not all of the different requirements may
be met at the same time. Also, the increasing use of
graphite-epoxy composites for the structural frames of an
aircraft postulates a new challenge to the drilling operation
[2]. Firstly, such materials are very tough, having a high
modulus, high strength and a very high stiffness per unit
weight. Secondly, improper drilling causes the delamination
of the graphite fibres which reflects in the poor quality of
the hole. The hole quality deteriorates with increasing
use of the drill and this can be critical to the life of
the riveted joints for which the holes are used.
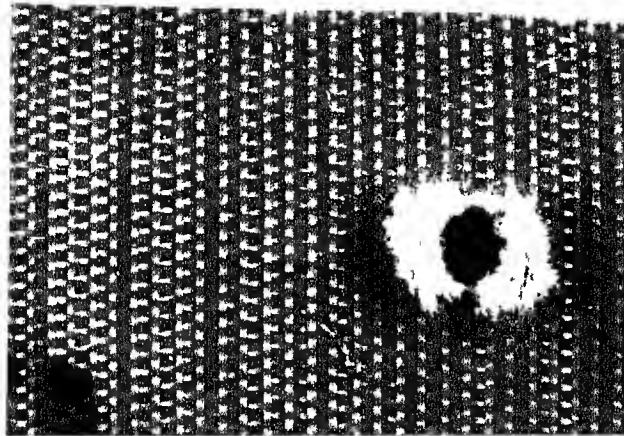
Photograph No. 1   Conventional Drilling of Kevlar-epoxy
                    Composite

Another serious problem of FRP machining is the generation of airborne dust. Glass and carbon fibre compounds usually emit a fine powder like dust, whereas a fibrous dust is typical for the machining of aramid. In any case the dust has to be extracted and filtered carefully, Since otherwise serious hazards to health or machine tool damage may occur [1].

In view of these facts, the need for developing a new technique for machining of composites, that overcomes the present drawbacks, cannot be overemphasised.

1.3 ELECTROCHEMICAL DISCHARGE MACHINING (ECDM)

An advantage of ECDM is that it can be used for the machining of any non-conducting material [3] irrespective of its mechanical properties such as strength, toughness, hardness, etc. Therefore, the process is ideally suited for the machining of composites.

In this process, two electrodes, one of which is the tool of the desired shape, and the other a flat plate of much larger area than the tool, are immersed in an electrolyte with a certain distance (~30-50 mm) maintained between them. It has been observed that the sparking occurs at the tool-electrolyte interface above a certain voltage (30-60 volts). Now if the sparking tool is brought in contact with the work-piece, which is kept between the two electrodes, machining takes place.

1.4 LITERATURE SURVEY

No literature could be found on "ECDM of composite materials", while limited literature is available on ECDM process as such [3,7,10,11]. Almost all the processes, that are in use at present, for the machining of composite materials have been dealt with in [1] and [4] alongwith their relative merits and demerits.

The different techniques and processes identified with composite manufacturing are as follows:

- methods of cutting cured and uncured composites
- machining technology for routing, trimming, beveling, countersinking and counterboring
- drilling technology
- mechanical fastening
- joining technology, which includes welding, adhesive bonding, brazing and diffusion welding
- coatings, e.g., paint and special coatings for protection against lighting and electromagnetic interference.

Schwartz [4] gives an interesting analysis of the conventional drilling of composites. In a conventional drill the neutral rake scrapes the material and causes it to resist penetration by the drill tip. It also tends to push the reinforcing fibres out in front, requiring a great deal of pressure to penetrate the piece. This pressure causes the

fibres to bend, resulting in furry, undersized holes. The pressure also produces excessive heat, which causes falling and chip clogging in the resin. The release of pressure as the tool bit breaks through the part causes a sudden and momentary increase in feed rate. As the tool plunges through the last few fibres, the cutter shaft, not the cutting edge, removes the remaining material. The result is chipping and cracking. The best way to analyze a drilling operation is to examine the chips. If the speed of the cutting tool is too high, heat will make the resin sticky and produce a lumpy chip; if the cutting edge is scraping and not cutting the plastic, the chips will be large and flaky. Either type will eventually clog any evacuation system.

The main problem of drilling FRP is the quality achieved at the tool exit side [1]. Therefore, the width of the damaged zone on that side and the surface roughness have been taken as the best indicators for the drilling result. The quality and the variation of measured values have been shown to be highly dependent on fibre orientation. Also the forces for the drilling of carbon-HT composites are found to be higher than for E-glass reinforcement, as long as the laminate structure is comparable [1]. In order to drill AFRPs orderly the fibres should be preloaded by tensile stress and cut in a shearing motion. It is therefore necessary to pull the fibres from the outer tool periphery towards the centre of the material. This requirement can be

met by tools with protruding peripheral cutting edges and positive radial and axial rake angles [1].

For trim routing glass-and carbon fibre compounds tools with multiple cutting edges made of cemented carbide or polycrystalline cutting materials are recommended [1]. The best machining quality is achieved by upmilling, independent of tool geometry and cutting conditions. Similar to drilling, the amount of cutting force and the surface quality in routing is very much dependent on fibre orientation.

Conventional routing tools with a unidirectional twisted helix are not suited for the routing of AFRP because fuzzing occurs due to axial cutting forces at the top layer which is not backed by adjacent material layers [5]. A straight flute design achieves a high machining quality at first, but after a very short cutting path rapidly increasing fuzzing occurs at both top layers [5].

Circular sawing uses diamond blades for most composite materials [4]. Cutting speed for composites normally varies from 2000 to 10,000 ft/min. Thicker parts are cut at proportionally lower feed rates. Saber sawing normally cuts Kevlar-epoxy with a blade which cuts the outermost fibres on both sides of the laminate towards the interior. Blade speeds of 2500 strokes per minute are recommended, but blade speed and feed rates may vary with material thickness.

Reciprocating-knife cutting is another technique used for the cutting of composites. There are two type of systems,

both of which incorporate high-speed reciprocating knives that are driven through the material to be cut by a mini-computer controlled, xyzc positioning system. In one system the cutting knife penetrates through the material into closely packed plastic bristles that constitute the surface of the cutting table. The system cuts in chopping mode, i.e., the knife rises above and plunges through the material onto the table. The second system can cut desired patterns in a continuous line at high speed. Curves, sharp corners, and notches can also be cut without lifting the knife from the material. Cutting results for both system indicate that the slicing and chopping system can cut a greater number of glass-epoxy and graphite-epoxy plies at twice the feed rate of the chopping system.

A widely used technique for the machining of FRP is water jet cutting (WJC) [6] . From the physical point of view, the water jet has good preconditions for cutting FRP. Especially thermal material damage is completely avoided. For contour cutting operations, which are very common in FRP machining, the almost point sized "tool" geometry and the multidirectional cutting ability of WJC are favourable.

Inspite of these advantages WJC has two major drawbacks [1]:

(i)   perpendicular to its own axis the jet has only limited stability and may therefore easily be distorted within

the cutting kerf. Due to this the cutting front, which is visible at the cut surface as a bundle of parallel grooves, is bent opposed to the feed direction. If the jet hits an obstacle, for example a fibre embedded in matrix, it will be deflected and will erode the "soft" components of the material first. Therefore FRP surfaces cut by water jet show that typical appearance of "washed out" matrix and protruding fibres. At the cutting limit the jet will erode matrix material only and will "jump" clearly visible and audible across the fibres, which remain as solid links across the kerf.

(ii) the jet force acts in the direction of the fluid flow and therefore generally perpendicular to the surface. This force direction, however, as pointed out earlier, is mainly responsible for material damage at the tool exit side. Additionally, the cutting process at the bottom of the kerf is slowed down due to the fact, that power density and therefore penetration ability has been absorbed by the layers above. This results in cracking and chipping at the exit side. The feed rate attainable is therefore in general limited by the surface quality required rather than the rough cutting ability of the jet.

Next to WJC the laser cutting technique is well suited for the contour trimming of FRP [1] . In general, aramid fibres are well, glass fibres less and carbon fibres hardly suited for laser cutting. This technique requires very precise control of focus position, feed rate and process gas flow. Especially this later parameter is, next to the power density and the intensity profile, the most important factor for the thermal damage of the material. Thermal damage is one major drawback of the laser technique besides the generation of smoke and fume. Surface quality and kerf geometry especially for thin laminates are very good, if single mode laser are used [1].

Cook, Foote, Jordan and Kalyani [3] have studied the discharge machining of glass. The process is shown to be electrolyte sensitive, and also varies somewhat with polarity. Further, for a given voltage, the rate of machining decreases with time. Machining rate increases both with concentration and temperature of electrolyte. Machining occurs more readily at corners. A pulsed d-c voltage supply was also used to test the effect of high frequency pulsed current [3]. It is found that for pulses in the milli-sec range, the removal rate is comparable to the d-c rate, while for pulses in the micro-sec range, rates increase by a factor of two. More striking is the effect of pulsed power (milli-sec or micro-sec) on the surface finish of the holes. The surface produced by pulsed power is found to be much smoother than that from a d-c supply. A variety of non-conductors have been tested and

machined successfully. Most of the results published by Cook et al. have been confirmed by Kumar [7].

A special mention needs to be made about the sparking in ECM. Larsson and Baxter [8] discussed about the reasons for sparking in ECM. For sparking to occur, metal to metal contact does not seems to be necessary. The onset of sparking coincided with the formation of large flat bubbles which blanketed a much larger area of the electrode than the more spherical bubbles. The sparking between electrode and solution could be clearly seen if two wire electrodes are held just touching on to the surface of a static electrolyte with a voltage of 100 volts or more. Violent sparks can be produced particularly at the cathode although potential gradient is probably more important than the potential difference. In an ECM cell, if the cathode becomes covered with a layer of thin large area bubbles, the current will be conducted by streamers of electrolyte between the bubbles thus causing a high potential gradient. Larsson, et al. further say that the sparks observed per square mm. of tool could be an inverse function of the gap, and the number of sparks decreases after sometime as the process proceeds. According to Loutrel and Cook [9] fields in the order of 10^6 volts/cm are generally required to produce field emission arcs in dielectrics. For the case of the electrolyte found in ECM, they theorize that arcs always form across voids. If the voltage gradient across the void

exceeds the dielectric strength or breakdown voltage, an
arc will occur. Once an arc is initiated, it may either
die or grow larger. After an arc is initiated, the heat
produced will begin to vaporize the surrounding electrolyte
causing the void to grow larger. If the voltage gradient in
the surrounding electrolyte is high, as in extreme machining
conditions, the arc will continue to grow, bridging the gap
and causing melting of the electrode surfaces. This is a
typical failure point in ECM. Loutrel, et al. have suggested
following seven mechanisms leading to high voltage gradients
in the presence of voids:

(1) Electrolytic gas evolution at electrode surfaces

(2) Depletion layers

(3) Electrode passivation and activation overvoltages

(4) Local stagnation of flow

(5) Steam generation and cavitation

(6) Vapor blanketing of electrode surface

(7) Particles in electrolyte flow.

Khayry and McGeough [10] have discussed metal removal
in the leading and side-gaps of ECDM drilling (for a conducting
workpiece). Electrochemical dissolution (ECD) and electrodischar
erosion (EDE) are shown to occur as discrete phases of randomly
varying intensity and duration. The random occurrence of
spikes in both working voltage and machining power that arise
during the ECD and EDE phases is described in terms of stochastic
difference equations which are obtained from the dynamic data

systems (DDS) modelling method. The special moments of the voltage and profiles developed from these models are used to discriminate between the phases of ECD, and the occurrence of arcs and sparks in machining gap. The analysis of machining power is shown to be useful only for qualitative assessments.

Crichton and Mc Geough [11] have used high speed photography to show that both spark and arc discharges are possible in an electrolyte. Further it is shown that the type of discharge may be distinguished from the energy of emitted radio frequencies or by the study of the light emitted. According to them on application of a voltage pulse between two electrodes immersed in an electrolyte, three phenomena may occur: (a) electrochemical action only, (b) electrochemical action followed by discharge between an electrode and the electrolyte, and (c) electrochemical action followed by discharge between the electrodes. Within the single pulse voltage and current waveforms obtained with phenomenon (c), four electrical stages may be distinguished:

> (1) high frequency oscillation (170 KHz),
> (2) high rate ECM,
> (3) low rate ECM, and
> (4) electrical discharge.

Stage 1 represents an unproductive period, however further work by the authors has shown that it may be eliminated by circuit modification. Stages 2 and 3 together represent an ECM phase, and stage 4 an EDM phase. The durations of these phases

respectively increase and decrease with increasing gap width and vary with electrolyte type, concentration and conductivity.

A comparison of ECDM with USM (ultrasonic machining) has been made by Kumar [7] . ECDM is reported to be having some distinct advantages over USM. The initial investment required for USM would be larger than that required for ECDM. The penetration rate of 2 mm/min obtained in ECDM is faster than the 1.5 mm/min obtained in USM (using a stainless steel circular tool of 1.6 mm diameter). Moreover the surface roughness of about 0.3 microns obtained with ECDM is also smaller than 0.5 microns obtained with USM(for a glass workpiece). Also it is found that with a rectangular tool the corners are less rounded with ECDM.

1.5 PRESENT WORK

From above literature survey it is evident that an efficient and accurate technique for machining of composites is not available. Conventional machining methods are associated with many drawbacks while laser cutting, apart from being inefficient, gives large heat affected zone. Water jet cutting, besides being expensive, has limited applications. But ECDM in which material removal rate is independent of mechanical properties of composites seems to be a potential composite material machining process.

For the present investigation an apparatus for ECDM was designed and fabricated in the laboratory. The feasibility of machining composite materials using this apparatus was studied. Glass-epoxy and Kevlar-epoxy laminates fabricated by hand-layup technique were used as work material. Two types of experiments were performed; cutting of glass-epoxy composites using a thin blade tool and machining of blind holes in Kevlar-epoxy composite using a solid circular tool.

Voltage, electrolyte conductivity, fibre volume fraction and tool diameter were taken as independent parameters. Their effect on material removal rate (MRR), tool wear rate (TWR), relative tool wear (RTW), and overcut produced was studied. The effect of sludge, that is produced during machining, on electrolyte conductivity was also investigated.

CHAPTER 2

EXPERIMENTATION

2.1 EXPERIMENTAL SETUP

A setup shown in Figure 2.1 was designed and fabrica-
ted. It consists of a tank/electrolyte and two electrodes,
                              of
one of which is a flat plate and the other is the tool of
the desired shape. Tool was made cathode and flat plate was
made anode.

Workpiece is held at a constant distance (~ 30 mm)
from the flat electrode which is a copper plate of about
75x75 mm and 1.6 mm thick. Gravity type feed mechanism is
provided for the workpiece. Dovetail guide-slide arrangement
is made for giving movement to the tool. A bridge rectifier
consisting of four diodes supplies the dc voltage between
the two electrodes, that can be regulated through a variac.

An overall view of the apparatus is shown in photograph
No.2.

2.2 SPECIMEN PREPARATION

6 mm thick composite plates were fabricated using
Kevlar-49 fabric (areal density 0.19 kg/m^2). This fabric
has the fibre volume ratio in warp and fill direction as
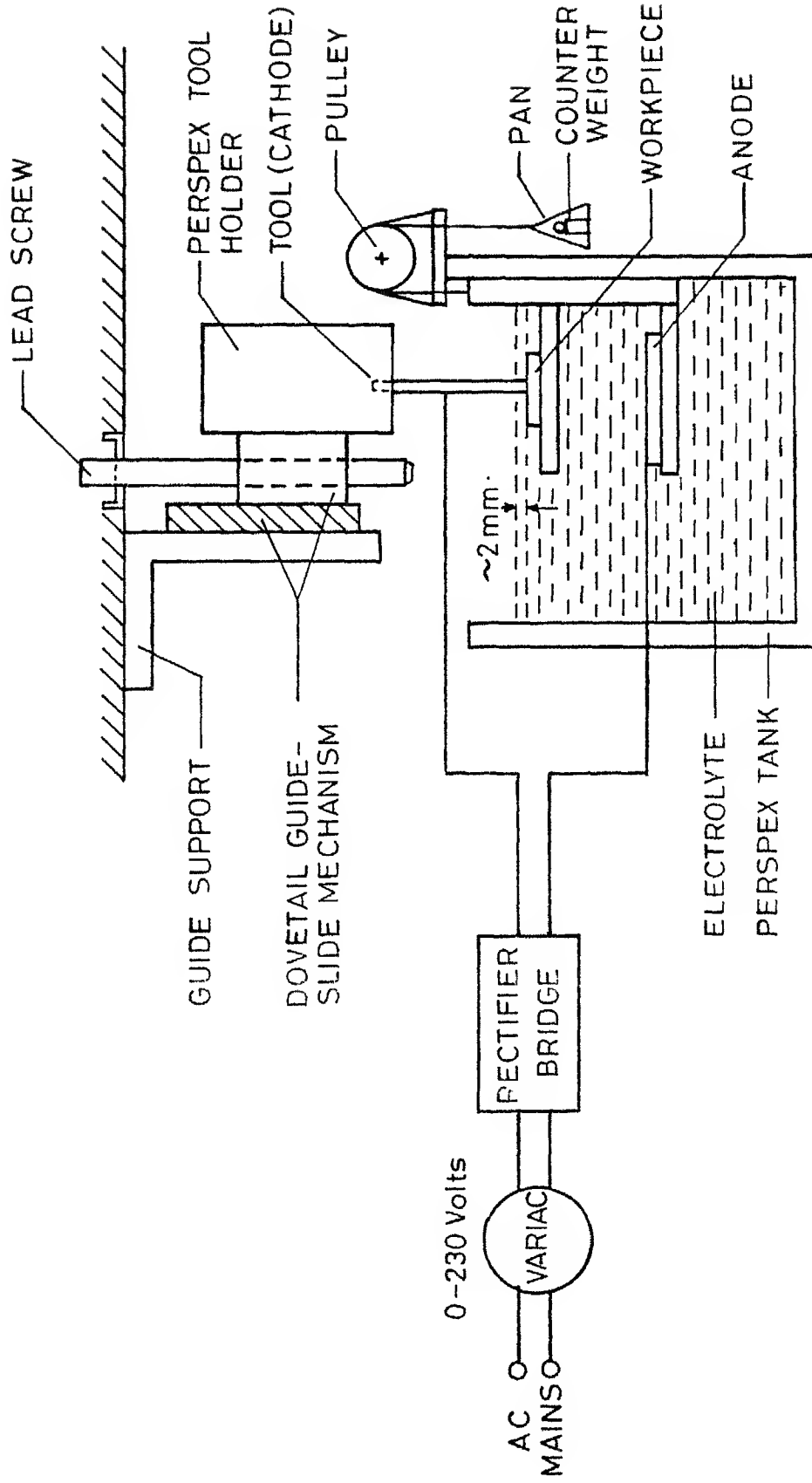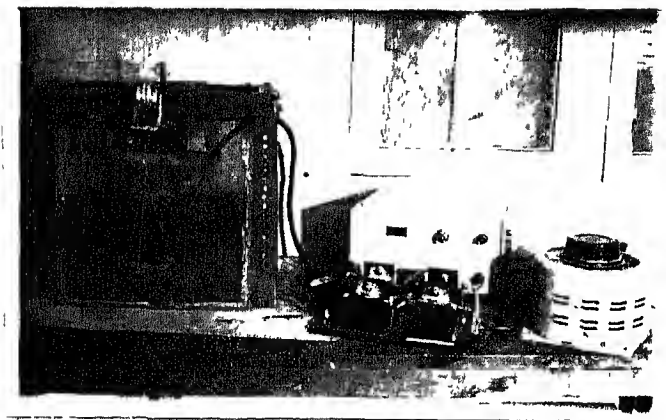10:1.

FIG. 2.1 SCHEMATIC DIAGRAM OF ECDM APPARATUS

Photograph No.2   An Overall View of ECDM Apparatus

Composite laminates were cast between two 25 mm thick mild steel mould plates lined with mylar sheets. These sheets make it easy to release the laminate from plates and also ensure a good surface finish. Twenty fabric pieces, that had been cut to the required size and demoisturized earlier, were placed on the lower mould plate one by one. Resin was spread by a brush on lower mould plate and on the top of each fabric piece. The laminate was rolled gently with a rubber roller after placing mylar sheet on top. This squeezes out the entrapped air and the extra epoxy. The upper mould plate was then placed on the top. The mould plates were separated by mild steel spacers to control the thickness of the laminate. The plates were cured at room temperature for about 6 hours and then at 55-60°C for another 12 hours by heating the mould plates through several 250W heating elements placed on the outer surface of each mould plate. The rate of heating could be controlled through a transformer.

Specimens of size 40x50 mm were cut on a circular sawing machine. Unconventional side of a metal splitting fine teethed H.S.S. cutter was used at high speed ($\sim$30 m/s). Fibre volume fraction using Eq. 1 is calculated as 44% and density is obtained as 1294 kg/m^3 using 'rule of mixtures' [12].

$$V_f = \frac{A\ N\ d_{fa}/d_f}{A_t} = \frac{N\ d_{fa}}{td_f} \qquad (1)$$

where,

A : Area of composite laminate

N : Number of CSM or Kevlar fabric layers in laminate

d_{fa} : Areal density of fabric/mat

d_f : Density of fibre

$$= 2.54 \times 10^3 \ kg/m^3 \ \text{for glass}$$

$$= 1.44 \times 10^3 \ kg/m^3 \ \text{for Kevlar}$$

t : Thickness of laminate.

Glass-epoxy composite plates of 3 mm thickness were also fabricated using hand layup technique. The procedure is same as above except for a few minor differences. Chopped strand mat (CSM) of glass fibres having an areal density of 0.6 kg/m^2, an average fibre length of 50 mm and manufactured by FGP Ltd., India was used. The matrix material was an epoxy resin commercially designated as Araldite LY 556 cured with 10% by weight of hardner HY 951, both supplied by Ciba-Geigy of India Ltd.

Five different plates were fabricated, each containing 3,4,5,6 and 7 layers of CSM, respectively. Fibre volume fractions for these five plates were calculated from Eq. 1 as 23.6%, 31.5%, 39.4%, 47.2% and 55.1%. Their densities, obtained experimentally using specific gravity bottle, were 1453, 1550, 1642, 1753 and 1843 kg/m^3.

Specimens of 50x9 mm were cut out of these plates for experimentation.

2.3   ECDM OF GLASS-EPOXY COMPOSITE

2.3.1 Experimental Procedure

Number of experiments were performed according to "design of experiments" technique [13,14] . Voltage, electrolyte conductivity and fibre volume fraction were considered as controll able variables and their effects on material removal rate (MRR), tool wear rate (TWR), relative tool wear (RTW) and overcut produced were studied. Table I gives the values of factors for different levels:

TABLE I

Values of X_1, X_2 and X_3 for Different Levels

| Factors | Symbol | LEVELS | | | | |
		-2	-1	0	1	2
Voltage (volts)	X_1	60	65	70	75	80
Fibre volume fraction (%)	X_2	23.6	31.5	39.4	47.2	55.1
Specific conductance (milli-mho/cm)	X_3	150	160	170	180	190

The scheme of experimentation and the responses obtained are given in Appendix A.

Each experiment was carried out for 15 minutes with machining being stopped after every 3 minutes. This was done to check the specific conductance of the electrolyte which increased due to temperature rise and the formation of sludge. It was brought back to its original value by diluting the electrolyte.

Tools were made of brass sheet about 0.6 mm thick. Each tool was approximately 15 mm in height, having a cutting edge of about 12 mm. One such tool is shown in photograph No.3. Dimensions of all the tools were duly recorded since for each experiment a fresh tool was used. During machining, tool was kept in contact with the workpiece and 2-3 mm below electrolyte level. Voltage was controlled by a variac and specific conductance was monitored with a digital conductivity meter (Systronics India Ltd.). Electrolyte used was NaCl.

Material removed from the workpiece and the tool was calculated by recording their initial and final weights on a single pan microbalance (accuracy of 0.00001 gm). Overcut was plotted/traced with the help of a shadow graph taken at a magnification of 20X (Figure 2.2). Some of the actual shadow graphs are shown in Appendix F. RTW was calculated as

$$\text{RTW} \atop (\% \text{ volume}) = \frac{\text{TWR}/d_t}{\text{MRR}/d_s} \times 100 \qquad (2)$$

Photograph No.3   Different Tools Used for Experimentation
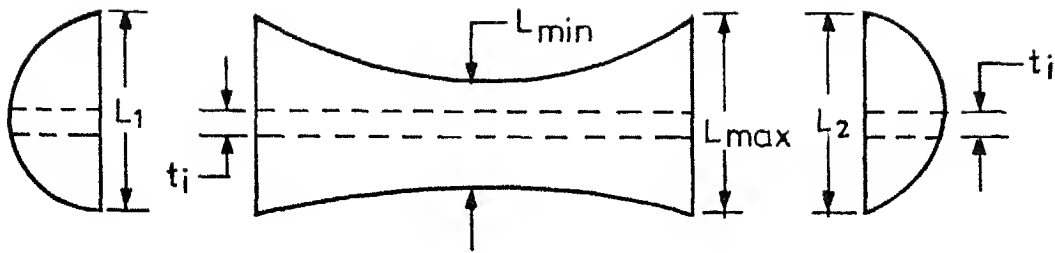
AVERAGE OVERCUT, $O_a = \dfrac{L_{max} + L_{min}}{2} - t_i$

TOP OVERCUT, $O_t \quad = \dfrac{L_1 + L_2}{2} - t_i$

WHERE,
   t_i IS THE THICKNESS OF THE TOOL
   USED IN i^{th} EXPERIMENT

FIG. 2.2 A TYPICAL SHADOW GRAPH OF THE MACHINED
         PROFILE.

d_t is the density of tool material

$= 8522 \text{ kg/m}^3$ for brass (70% Cu, 30% Zn) [15]

d_s is the density of specimen.

The responses thus obtained were fed to a computer program CADEAG-1 [16] to get the relationships between different parameters and responses. Additional experiments, Table A-2, Appendix A, were performed to check the validity of the model.

2.3.2 Design of Experiments

Accordingto Adler, Markova and Granvosky [14] the design of an experiment is the procedure for selecting the number of trials and conditions for running the experiments, essential and sufficient for solving the problem that has been set with the required precision. The important features are as follows:

(a)   the simultaneous variation of all the variables
        determining a process according to special rules called
        algorithms;

(b)   striving to minimize the total numbers of trials and,

(c)   the selection of a clear cut strategy permitting the
        experimenter to make substantial decisions after
        each series of experiments.

A polynomial response surface equation of second order can be represented as,

$$Y_u \; = \; B_o \; + \; \sum_{i=1}^{K} \; B_i X_i \; + \; \sum_{i=1}^{K} \; B_{ii} X_i^2 \; + \; \sum_{i<j} B_{ij} X_i X_j$$

(3)

where Y_u is the response (MRR, TWR etc.) and $1, 2, \ldots, K$ are the coded levels of K quantitative variables or factors. The coefficients B_o, B_1, etc. are known as regression coefficients. The polynomial in Eq. 3 is also known as regression function. The first term under the summation sign pertains to linear effect, the second term pertains to the higher order effects and the third term pertains to the interactive effects of the parameters under investigation.

The actual values of the levels for the factors, X_1, X_2 and X_3 are shown in Table I.

2.4 MACHINING OF BLIND HOLES IN KEVLAR-EPOXY COMPOSITE

2.4.1 Experimental Procedure

Effect of specific conductance and tool diameter on MRR, TWR, RTW and overcut produced was studied. Experiments were conducted at a constant voltage of 75 volts and the electrolyte used was NaCl. Copper tools of diameter 2, 3, 4 and 5 mm were used (Photograph No. 3) and these were insulated at the sides with teflon tape. Again separate tools were used for each experiment. For a fixed diameter, specific conductance was varied in steps of 10 from 110 milli-mho/cm to 140 milli-mho/cm and the responses measured, as in Section 2.3.1, are

given in Table D-1, Appendix D. For calculating RTW, the value of d_t used in Eq. 2 was 8954 kg/m^3 [15] . The effect of moisture absorbed by Kevlar fibres during machining, if any, was ignored while calculating MRR. Overcut has been calculated as the diametral difference of hole produced and tool used and henceforth will be called as diametral overcut, O_d. The value of specific conductance was kept low to avoid the surface damage that occurred, probably due to low decomposition temperature of Kevlar fibres (500°C). Machining time varied from 20 to 45 minutes depending upon the diameter of the tool. The specific conductance was monitored at an interval of 5 minutes. Holes machined were 3-4 mm in depth.

2.5 EFFECT OF SLUDGE

As the machining progresses a brown precipitate called sludge is formed. Since no literature is available about its effect on electrolyte conductivity, this phenomenon was also studied.

For experimentation purposes, the sludge produced during machining was filtered and dried. 500 ml of NaCl electrolyte was taken in a beaker and its specific conductance recorded. The temperature of the electrolyte was then varied from room temperature to 60°C using a thermostat control and a

heating coil. Changed values of specific conductance were recorded at different temperature levels. This solution was then allowed to cool to room temperature. To this 10 gms of dried sludge was added and the solution was properly stirred. Again the reading of specific conductance was taken. Then the temperature was raised to 60°C in steps and appropriate values were recorded at each step. At 60°C another 10 gms of sludge was added and reading recorded after adequately stirring the solution. Again the solution was allowed to cool to room temperature and readings were taken at the intermediate values of temperature. This cycle was repeated by increasing sludge concentration in steps of 10 gms. upto a sludge concentration of 40 gms. in 500 ml of electrolyte solution.

Another experiment was conducted at room temperature wherein sludge concentration was varied from 0 to 50 gms. in steps of 10 gm. and observation made in one case by stirring the solution and in the other case in unstirred solution. The volume of NaCl solution taken was 500 ml.

CHAPTER   3

RESULTS AND DISCUSSION

## 3.1   CUTTING OF GLASS-EPOXY COMPOSITE

Here the results of ECDM of glass-epoxy composite
are presented. Using the responses, obtained experimentally
and given in Table A-1, Appendix A, response surface model,
Eq. 3, was evolved with the help of a computer program
CADEAG-1. Using these models effect of different factors
(voltage, specific conductance of electrolyte and fibre volume
fraction) on the responses has been studied and discussed below.
Few experimental points have also been shown in each graph.
It is seen that there is a good agreement between experimental
points and the curves derived from these models.

Some of the specimens as machined by ECDM are shown
in Photograph No. 4.

3.1.1   Material Removal Rate (MRR)

MRR is defined as the total material removed from
the work piece divided by the machining time.

The effect of voltage on MRR is shown in Figure 3.1
for two values of specific conductance (170 and 190 milli-mho/cm)
MRR is seen to increase with voltage and this effect is more
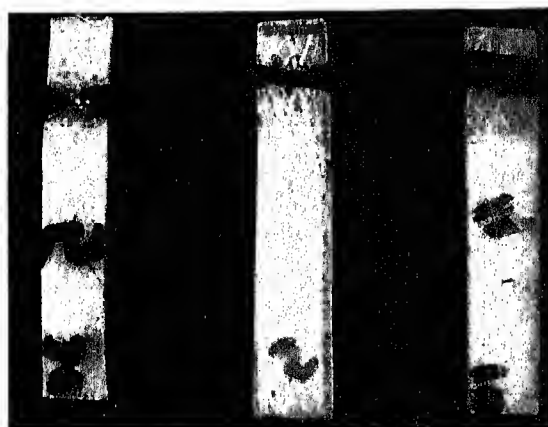
Photograph No.4   Glass-epoxy Composite Specimens Cut by
                   ECDM

pronounced above 65 volts. Increase in voltage implies higher discharge energy and hence more MRR.

From Table B-2, Appendix B, it is seen that the independent and higher order effects of voltage are highly significant. The interactive effect of voltage and specific conductance is also significant but to a lesser extent.

Effect of specific conductance on MRR is shown in Figure 3.2. An increase in specific conductance means increased electrolyte conductivity and consequently more electrolytic current. The process of electrolysis is accelerated by an increase in the electrolytic current. This results in a greater rate of hydrogen bubbles formation at the cathode surface. Since sparking occurs across the bubbles [8,9], an increased rate of H_2 bubbles formation implies enhanced rate of sparking and hence higher MRR. Therefore, MRR is found to increase with increasing specific conductance.

From Table-2 (Appendix B), independent effect of specific conductance is found to be highly significant while its higher order effect is insignificant. Specific conductance also has a significant interactive effect with voltage.

MRR is observed to decrease with increase in fibre volume fraction as is seen in Figure 3.3. Machining is presumed to proceed primarily by melting and vaporisation of work material. An increase in fibre volume fraction results in higher volume of glass fibres in a given volume of specimen. Now glass fibres have a melting point of about 1250°C which is

much higher than that of epoxy which has a decomposition temperature of 280°C. Therefore, an increase in fibre volume fraction will decrease MRR, other factors remaining constant.

From Table B-2 (Appendix B) it is evident that the independent effect of fibre volume fraction is significant though its higher order and interactive effects are insignificant.

3.1.2 Tool Wear Rate (TWR)

TWR is defined as the reduction in weight of tool during machining divided by the machining time.

Figures 3.4 and 3.5 show the effect of voltage and specific conductance on TWR, respectively. TWR is observed to increase with an increase in voltage and specific conductance. This is similar to the dependence of MRR on these two factors and the same reasoning, as given in Section 3.1.1, applies here also.

Table B-2 (Appendix B) shows that the independent effects of voltage and specific conductance are significant. But their higher order and interactive effects are seen to be insignificant.

TWR seems to be independent of fibre volume fraction (Figure 3.6). This is expected since work material does not influence tool performance in any way.

This fact is well supported by Table B-2 (Appendix B) from where it can be seen that all the three effects of fibre volume fraction (independent, higher order and interactive) are insignificant.

3.1.3 Relative Tool Wear (RTW)

From Eq. 2 (Chapter 2), it can be seen that RTW is directly proportional to TWR and inversely proportional to MRR. Therefore, the behaviour of RTW is determined by the relative effect of a parameter on TWR and MRR.

In Figure 3.7, RTW is shown to decrease with increasing voltage. Although, both TWR and MRR increase with voltage, the effect of MRR seems to be predominant in this case and hence the decrease in RTW.

From Table B-2 (Appendix B) it can be seen that the independent effect of voltage is highly significant while higher order effect is insignificant. The interactive effect of voltage and specific conductance is seen to be significant.

Figure 3.8 shows the variation of RTW with specific conductance. For similar reasons as discussed above, RTW is seen to decrease with increase in specific conductance, decrease being faster for lower values of specific conductance.

It is evident from Table B-2 (Appendix B) that the independent and higher order effects of specific conductance are highly significant. Also there is a significant interactive effect of specific conductance with voltage.

Figure 3.9 shows the effect of fibre volume fraction on RTW. Since TWR does not depend on fibre volume fraction while MRR decreases with it, RTW is observed to increase with increasing number of layers.

Table B-2 (Appendix B) shows that the independent effect of fibre volume fraction is significant though its higher order and interactive effects are insignificant.

3.1.4 Average and Top Overcut (O_a and O_t)

The dependence of average and top overcut (defined in Figure 2.2) on voltage is shown in Figures 3.10 and 3.13. The effect of specific conductance on average and top overcut is shown in Figures 3.11 and 3.14, respectively. During machining, work material is removed simultaneously by the front face as well as the side surface of the tool. Therefore, an increase in MRR also implies increased overcut. Thus, both average and top overcuts are found to increase with increase in voltage and specific conductance since MRR also increases with these two parameters.

From Table B-2 (Appendix B), it is evident that the independent effects of voltage and specific conductance on O_a and O_t are highly significant. Higher order effects of voltage and specific conductance are also seen to be significant for both O_a and O_t. In case of O_t, there is a significant

interactive effect between voltage and fibre volume fraction while in the case of O_a interactive effects are insignificant.

From Figures 3.12 and 3.15 it is seen that both average and top overcuts are independent of fibre volume fraction. Thus, overcut is a function of machining conditions only.

This is well supported by Table B-2 (Appendix B) from where it may be seen that the independent, higher order and interactive effects of fibre volume fraction on O_a and O_t are insignificant.

3.2 OPTIMIZATION OF MACHINING CONDITIONS

Figures 3.1 to 3.15 may be termed as the "operating characteristics" of the process and can be used to obtain optimum machining parameters.

Generally, overcut produced during unconventional machining process can be taken as a measure of the quality produced and therefore, can be treated as a constraint for the optimization problem.

For a given value of overcut, it would be of interest to know what is the fastest way of conducting machining or what are the cutting conditions for which RTW is minimum.

From Figure 3.10, it can be seen that for a fixed value of average overcut (O_a) there are different combinations of voltage and specific conductance. Each such combination of

voltage and specific conductance corresponds to unique values of MRR and RTW. Table II gives MRR and RTW values for these combinations, for varying fibre volume fractions, corresponding to an average overcut (O_a) of 2.26 mm. It can be seen from Table II that for a fixed fibre volume fraction there is an optimum combination of voltage and specific conductance that maximizes MRR. Another optimum combination can be the one that minimizes RTW. Let MRR^* and RTW^* be the optimum values of MRR and RTW that can be obtained for a given O_a and a particular fibre volume fraction.

MRR^* and RTW^* corresponding to different O_a's have been obtained and summarised in Tables C-1 and C-2, Appendix C.

These results have been plotted in Figures 3.16 and 3.17.

3.2.1   Optimum Material Removal Rate (MRR^*)

Figure 3.16 shows that the MRR^* increases linearly with increasing O_a.

For a given value of O_a and fibre volume fraction, it is possible to know the maximum MRR that can be achieved. From Table II, one may observe that though MRR^* decreases with increase in fibre volume fraction, the optimum cutting conditions (voltage, V^* and specific conductance, k^*) remain the same.

3.2.2   Optimum Relative Tool Wear (RTW^*)

Figure 3.17 depicts the relation between RTW^* and average overcut. RTW^* is seen to decrease with increasing O_a

TABLE II

MRR and RTW Values Corresponding to Different Cutting Conditions
for a Fixed Value of Average Overcut (O_a = 2.26 mm)

| | CUTTING CONDITIONS | | V_f = 23.6% | | V_f = 31.5% | | V_f = 39.4% | | V_f = 47.2% | | V_f = 55.% |
SL. No.	Voltage (volts)	Sp.conductance (milli-mho/cm)	MRR (mg/min)	RTW (%)	MRR (mg/min)	RTW (%)	MRR (mg/min)	RTW (%)	MRR (mg/min)	RTW (%)	MRR (mg/min)
1	70.00	190	6.06	2.48	5.72	2.64	5.46	2.75	5.27	2.79	5.17
2	73.75	180	6.42*	2.46	6.00*	2.62	5.61*	2.65*	5.30*	2.70*	5.19*
3	76.25	170	6.23	2.29*	5.71	2.52*	5.01	2.79	4.96	3.15	4.75
4	78.00	160	5.56	2.34	5.00	2.96	4.60	3.38	4.18	3.89	3.94
5	78.88	150	4.17	3.08	3.64	3.90	3.23	4.58	2.85	5.33	2.50

* indicates optimum valves

V_f : fibre volume fraction.

and this decrease is quite steep upto a value of 1.88 mm
(O_a). Beyond this value there is not much change in RTW^*.
From Table II it can also be seen that the optimum combi-
nation for RTW^* need not be the same as the one for MRR^*.

3.3   MACHINING OF BLIND HOLES IN KEVLAR-EPOXY COMPOSITE

Blind holes were drilled in Kevlar-epoxy laminates
using copper tools of varying diameters. Experiments were
conducted at different values of specific conductance while
the voltage was kept constant. Here, the effects of specific
conductance and tool diameter on MRR, TWR, RTW and diametral
overcut are discussed. Diametral overcut, O_d, is defined
as the difference in the diameter of hole produced and the
diameter of the tool used. Experimental results are recorded
in Appendix D. Machined specimens are shown in Photograph
No.5.

3.3.1   Material Removal Rate (MRR)

MRR increases with specific conductance as shown in
Figure 3.18. The reasons for this behaviour are the same
as discussed earlier in Section 3.1.1.

The effect of tool diameter on MRR is shown in
Figure 3.19. It is observed that with an increase in diameter
there is a decrease in MRR. An increase in diameter results in
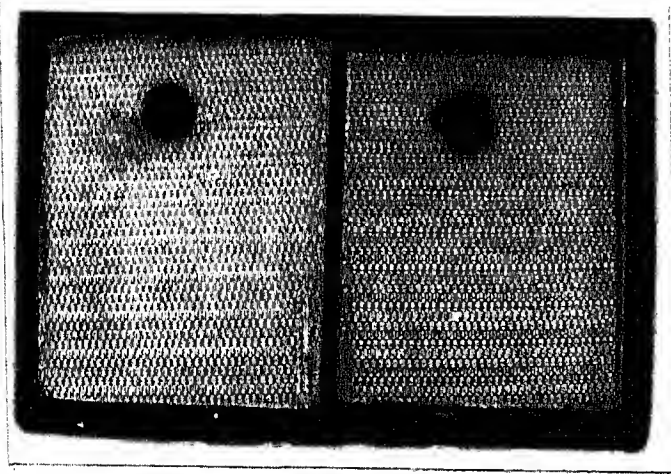
Photograph No.5   Blind Holes in Kevlar-epoxy Composite
                   Machined by ECDM

lower current density and there will be lesser sparks per
unit area. This will mean reduced spark intensity which
can result in lower MRR. This could be observed visually
also. Sparking in the case of 2 mm diameter tool was seen
to be very intense in comparison to 5 mm diameter tool.

3.3.2 Tool Wear Rate (TWR)

TWR is observed to increase with specific conductance
(Figure 3.20), as in Section 3.1.2.

Figure 3.21 shows decrease in TWR with increase in
tool diameter. This is due to the same reasons as discussed
above in Section 3.1.2. At 140 milli-mho/cm, change of diameter
from 2 to 5 mm results in 60.8% decrease in TWR, while at
110 milli-mho/cm it results in a 77.7% reduction in TWR.

3.3.3 Relative Tool Wear (RTW)

RTW increases with increase in specific conductance
as is shown in Figure 3.22. RTW is directly proportional to
TWR and inversely proportional to MRR. Further, both TWR
and RTW increase with specific conductance. Therefore, when
specific conductance is increased the effect of MRR will be to
reduce RTW whereas TWR will tend to increase RTW. Since RTW
is increasing with specific conductance it implies that
the effect of TWR is predominant. This is well supported by
the fact that an increase in specific conductance from 110 to 140
milli-mho/cm, for a 2 mm diameter tool, resulted in a 113%

increase in TWR compared to a 35.6% increase in MRR (Figures 3.18 and 3.20).

In Figure 3.23, RTW is found to decrease with increasing diameter. Both TWR and MRR decrease with diameter. Therefore, using the same reasoning as above one can conclude that the effect of TWR is predominant.

3.3.4 Diametral Overcut (O_d)

Figure 3.24 shows increase in diametral overcut with specific conductance. Cutting occurs both at the side surface and front face of the tool. Since MRR increases with increase in specific conductance the same is observed for diametral overcut also, as discussed earlier in Section 3.1.4.

Since MRR decreases with increasing diameter (Section 3.3.1) therefore, diametral overcut is also found to decrease with increase in tool diameter (Figure 3.25).

3.4 EFFECT OF SLUDGE

During machining, a brown precipitate called sludge starts forming at the top surface of the electrolyte. As the machining progresses this precipitate starts settling down towards the bottom of the tank while still more of it is formed at the top.

Figure 3.26 shows the effect of sludge concentration on the specific conductance of electrolyte. The curves have been plotted for two different conditions, i.e. when the

solution is properly stirred and when it is left undisturbed
(i.e., unstirred). Since the rate of settling down of
the sludge is very slow, as observed visually, the effect of
sludge concentration during machining will lie between the
two curves shown in Figure 3.26. Though the actual composition
of sludge is not known, its effect on specific conductance
shows that it consists of conducting compounds. These may
be the products of electrolysis, hydroxides of copper (which
is the anode material) and sodium, traces of tool material
and its compounds. Besides there may be traces of non-conducting
work material and their effect, if any, will be to lower the
conductance of sludge.

Figure 3.27 shows the effect of temperature on specific
conductance. A linear relationship is observed. Figure 3.28
depicts the nature of specific conductance vs. sludge concen-
tration curve for different temperatures. Specific conductance
is found to increase with sludge concentration but the relation-
ship is non-linear.

The experimental results are recorded in Tables E-1
and E-2, Appendix E.
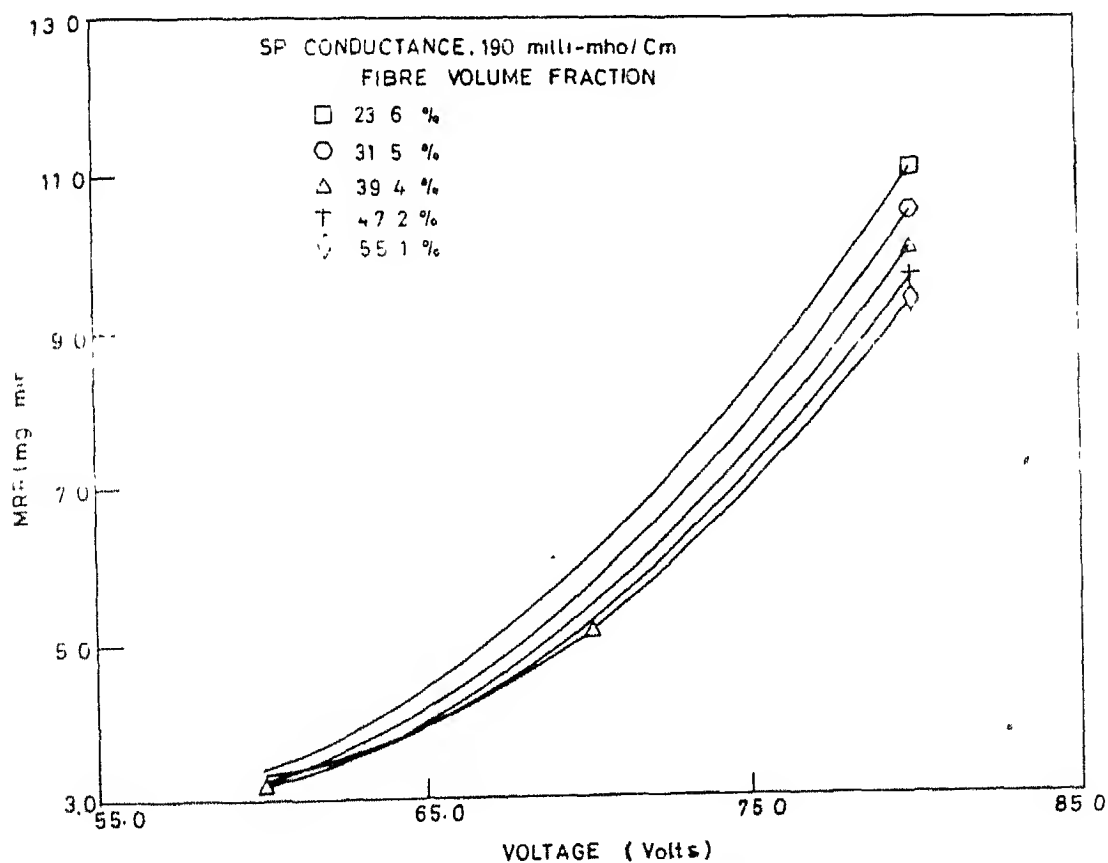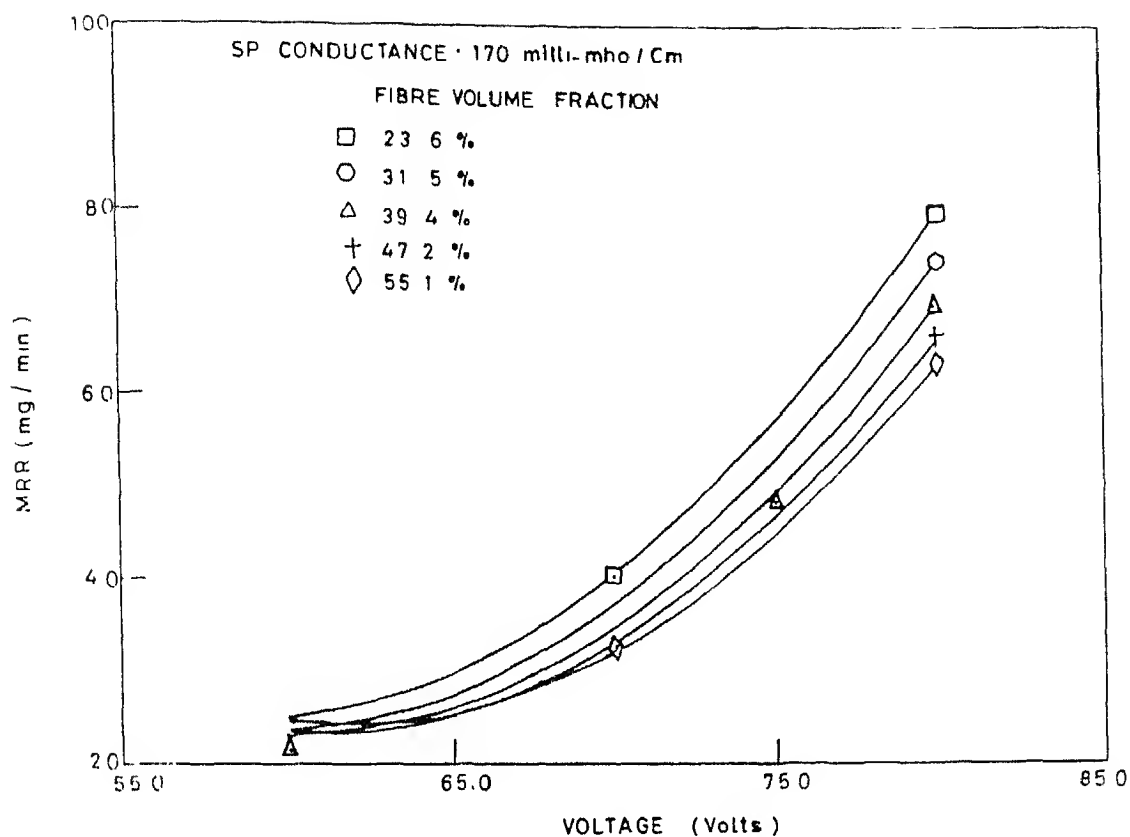
FIG. 3.1 EFFECT OF VOLTAGE ON MRR
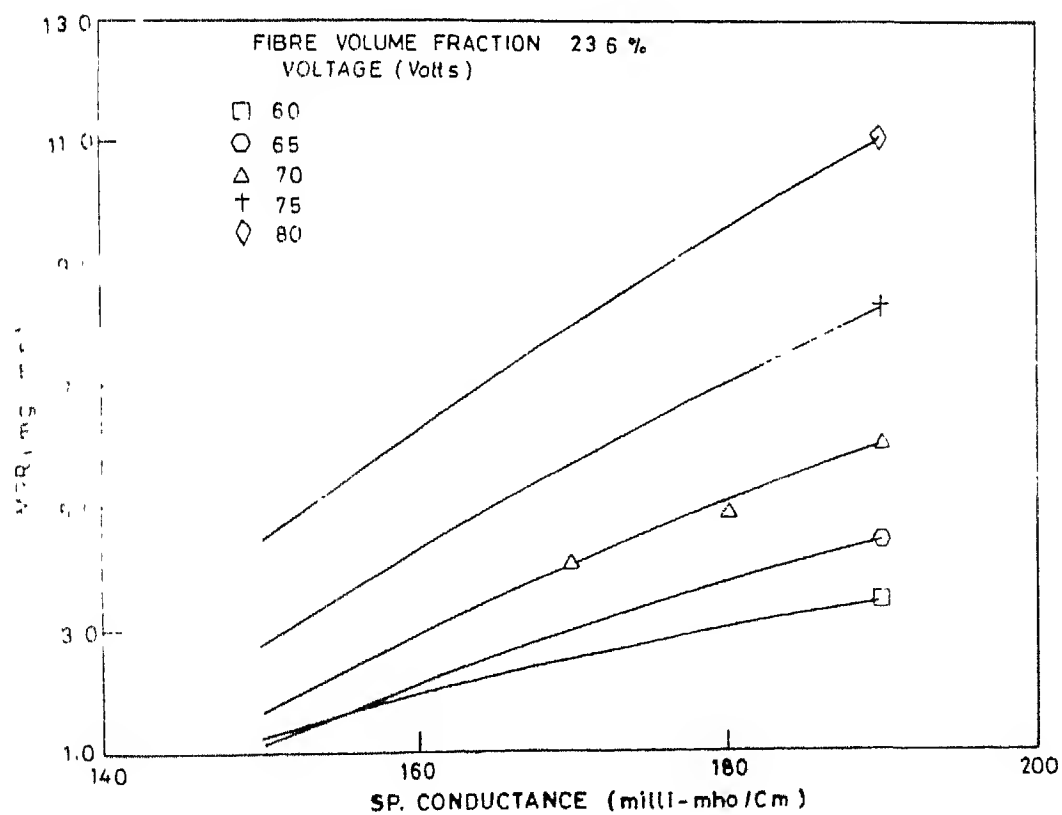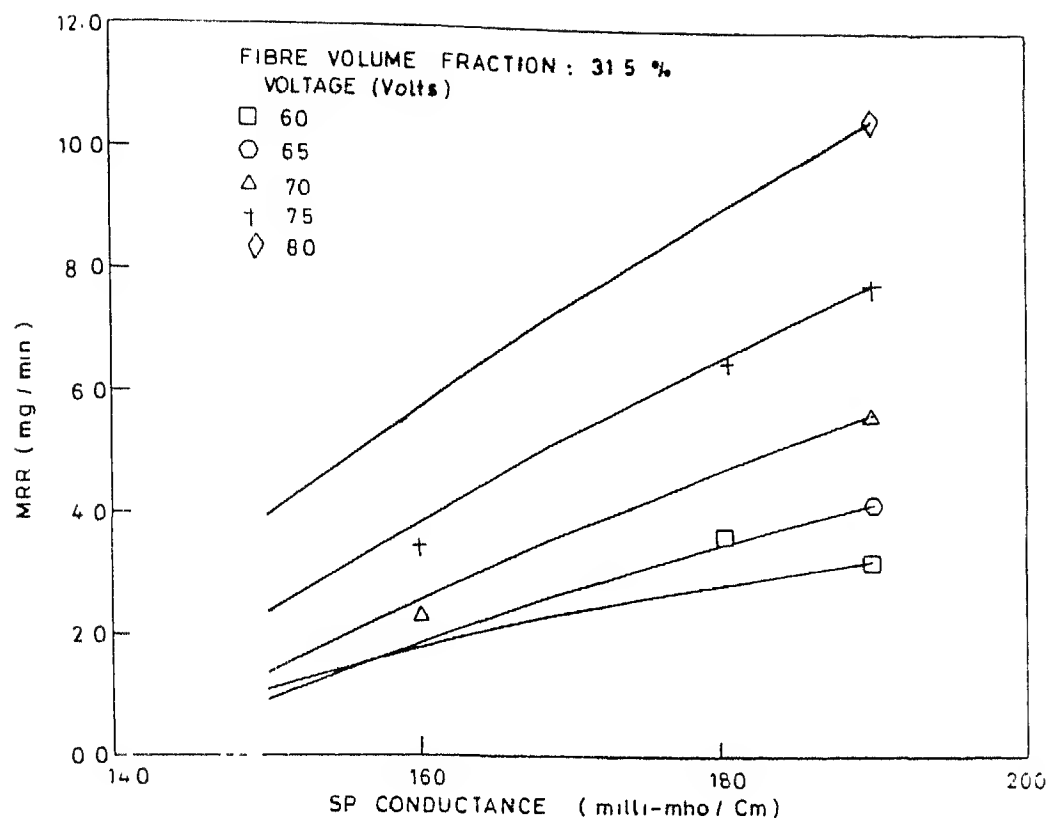
FIG.3.2 EFFECT OF SP. CONDUCTANCE ON MRR
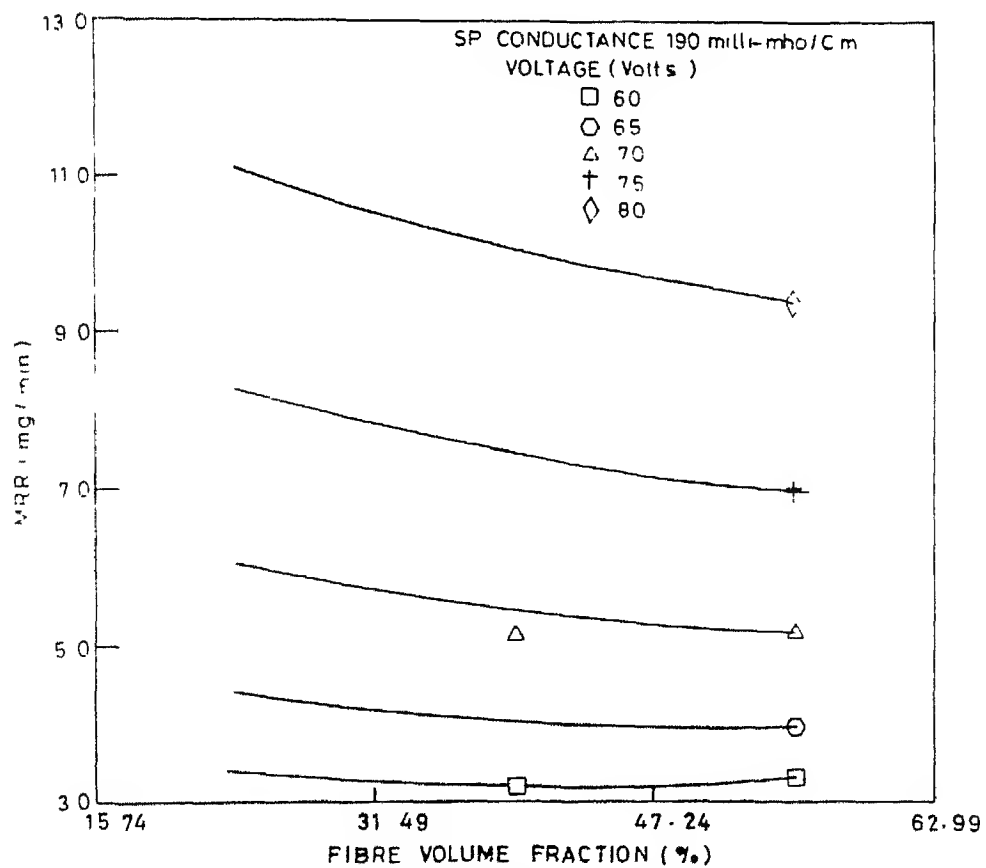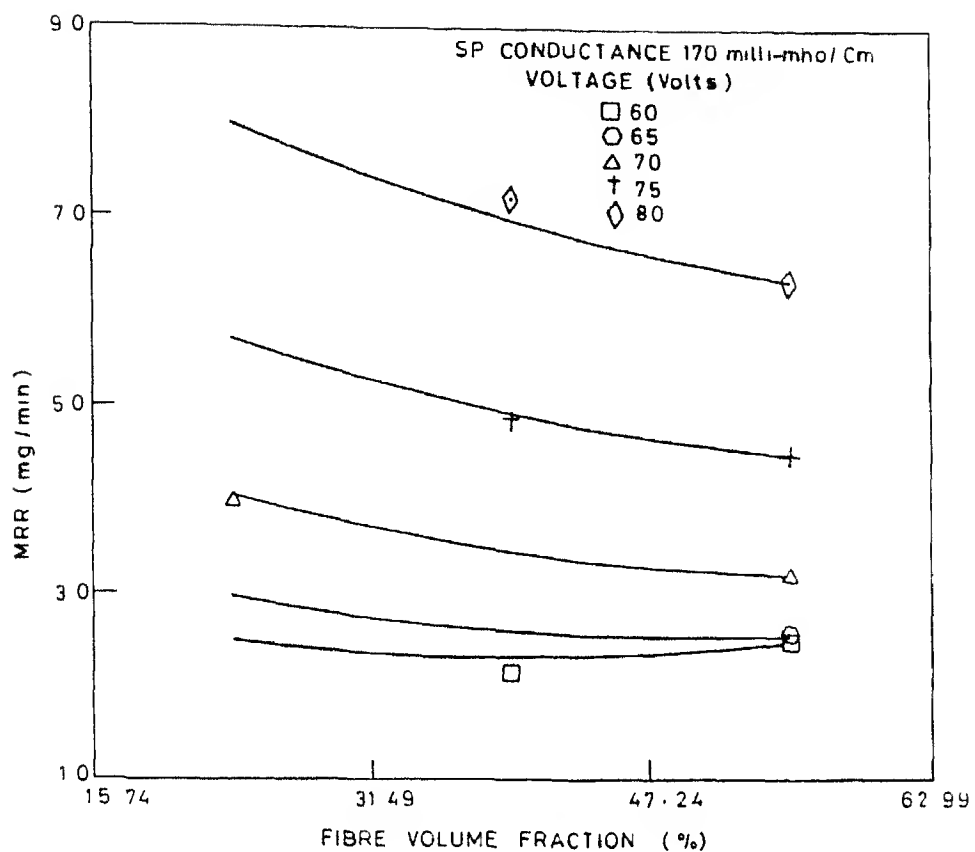
FIG.3·3 EFFECT OF FIBRE VOLUME FRACTION ON MRR
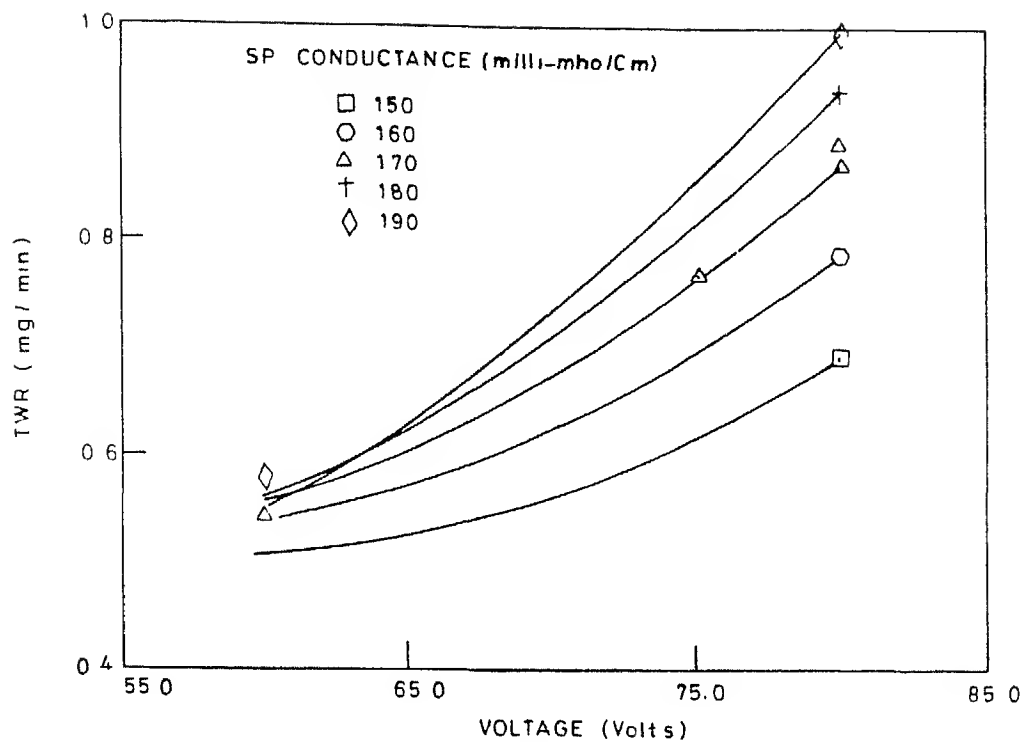
FIG. 3.4 EFFECT OF VOLTAGE ON TWR
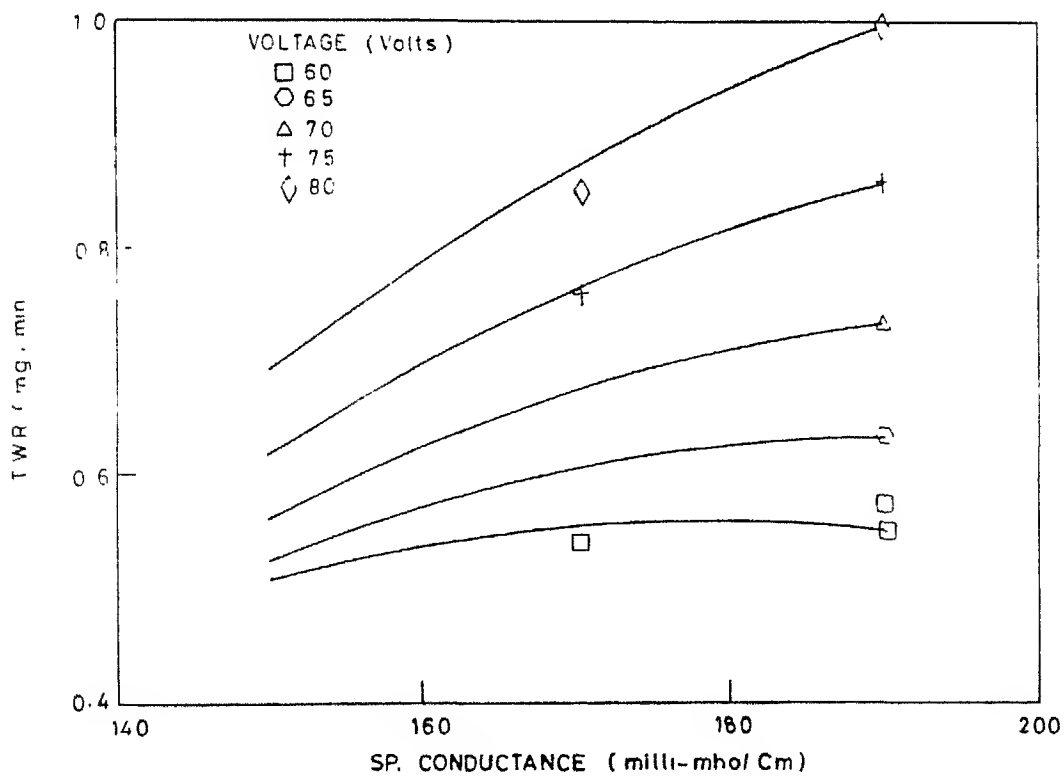
FIG. 3.5 EFFECT OF SP. CONDUCTANCE ON TWR
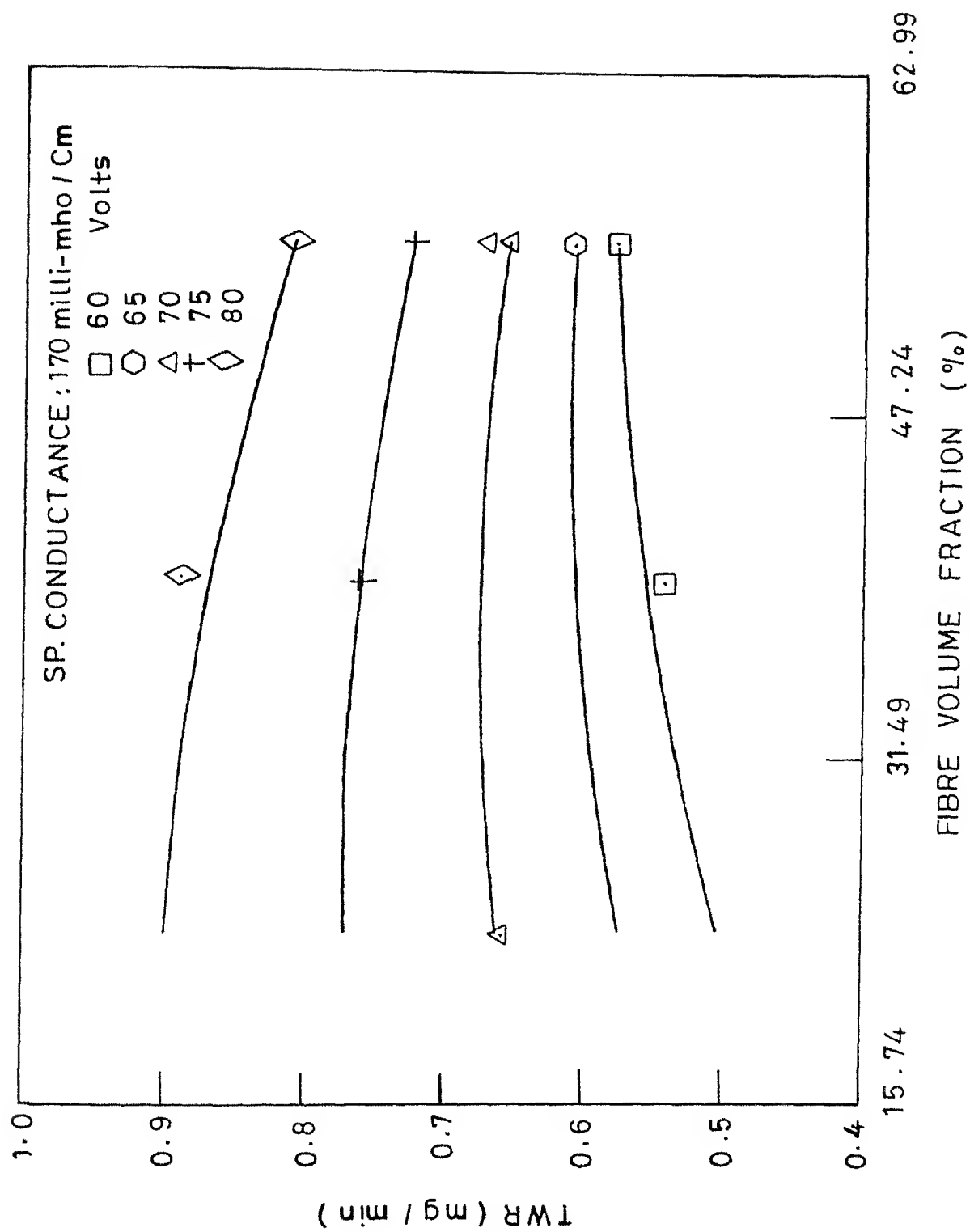
FIG.3.6 EFFECT OF FIBRE VOLUME FRACTION ON TWR
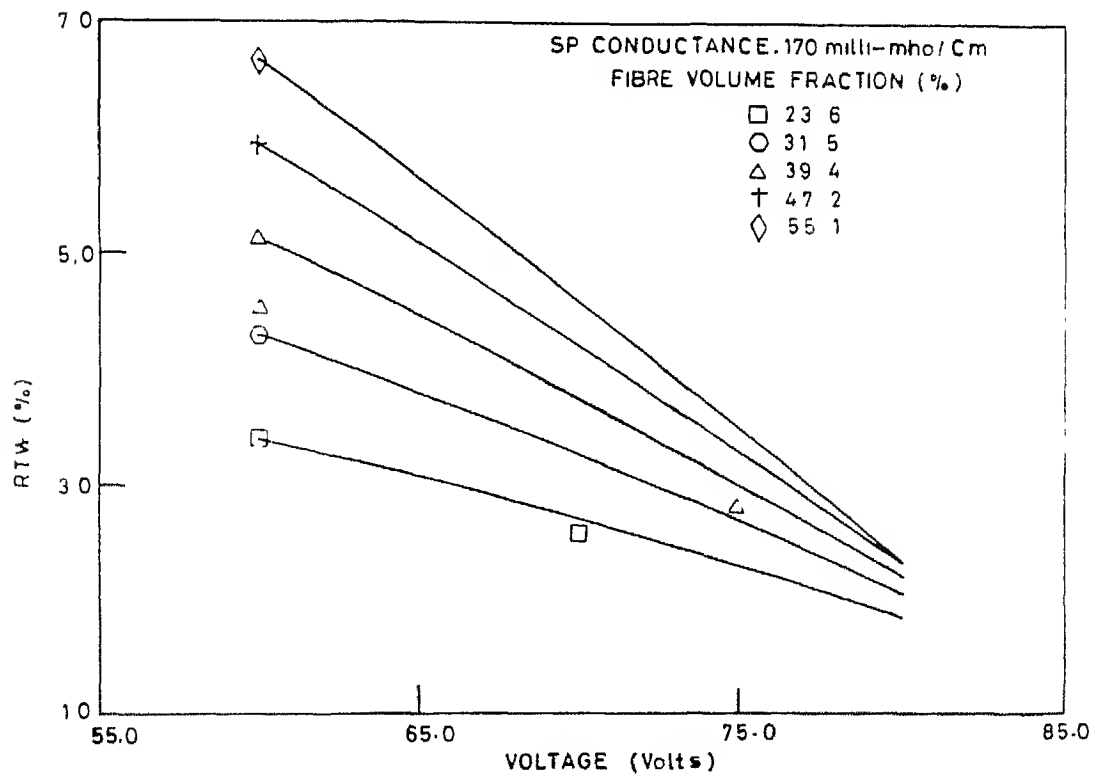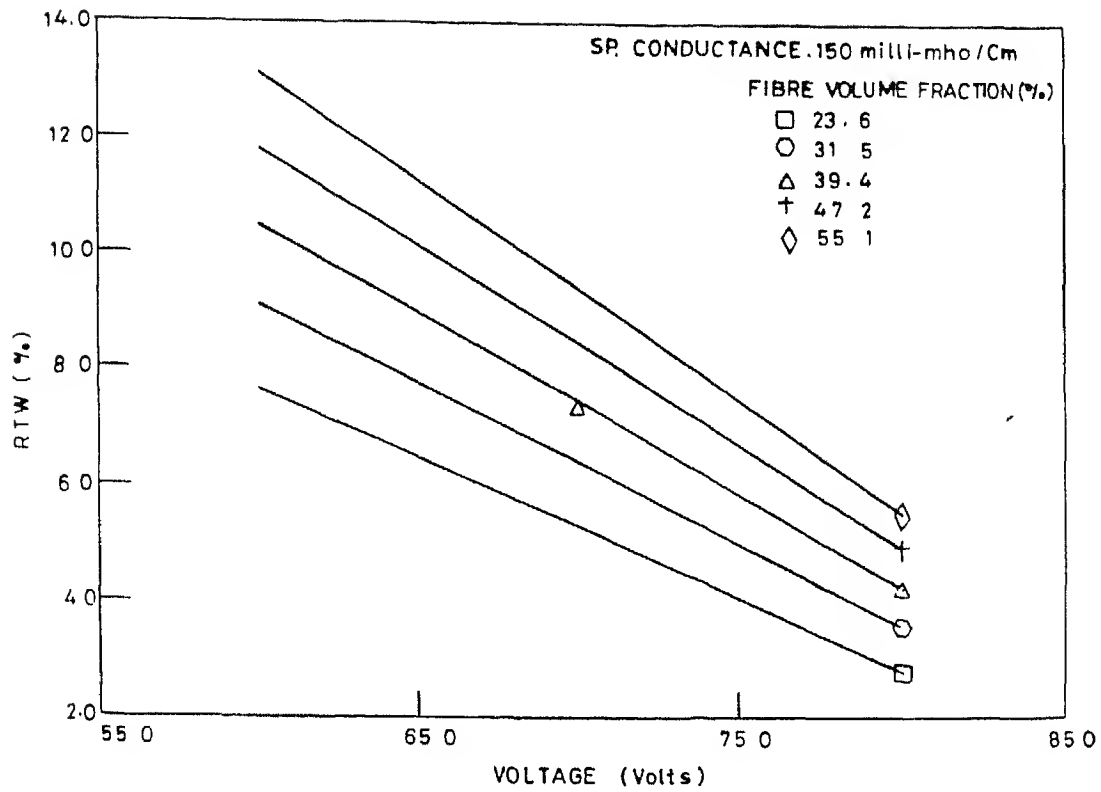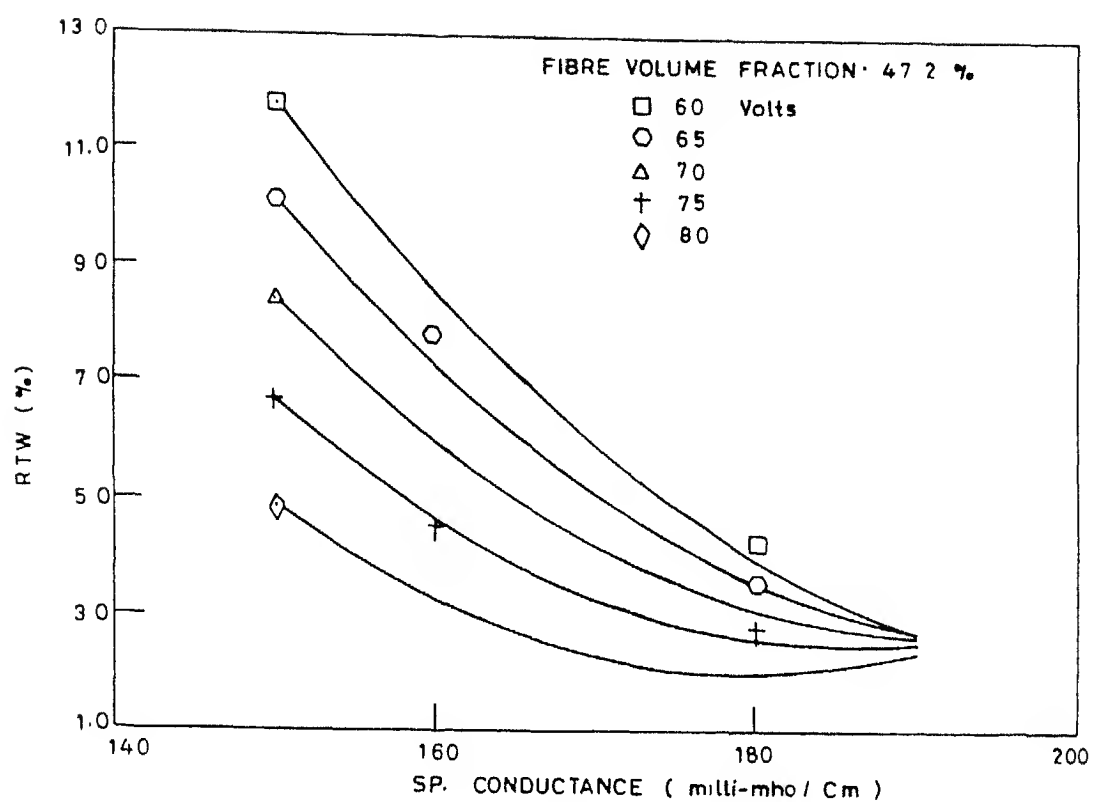
FIG. 3.7 EFFECT OF VOLTAGE ON RTW
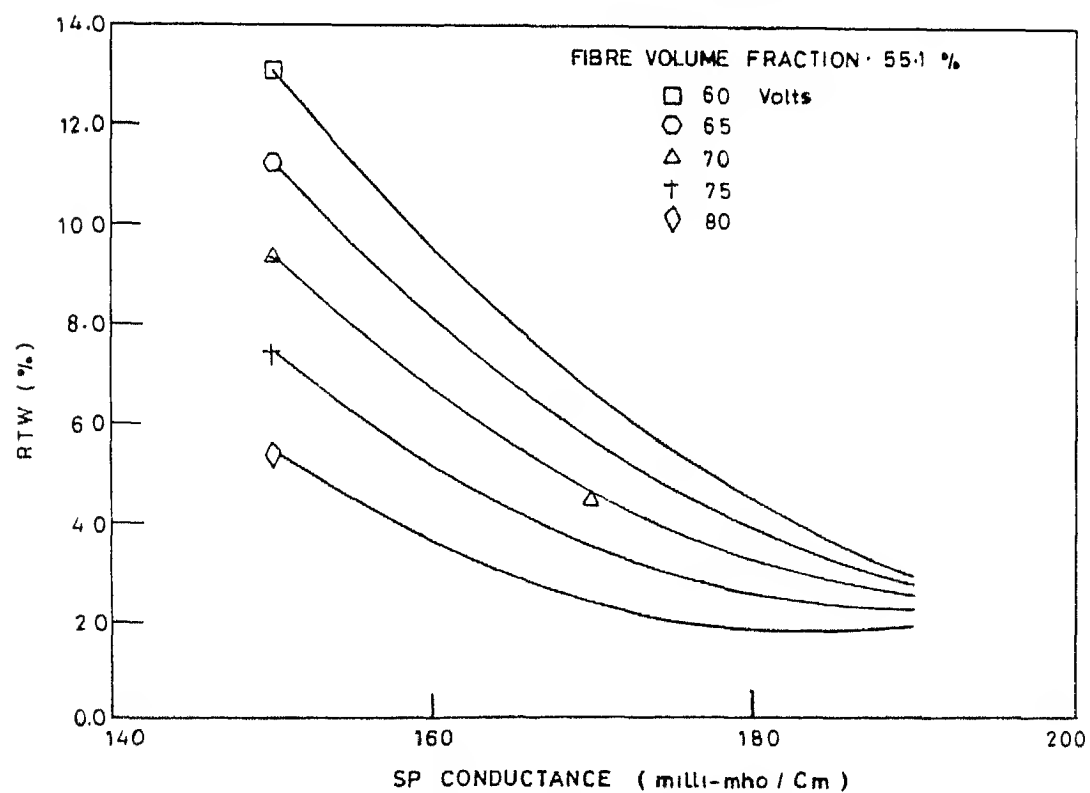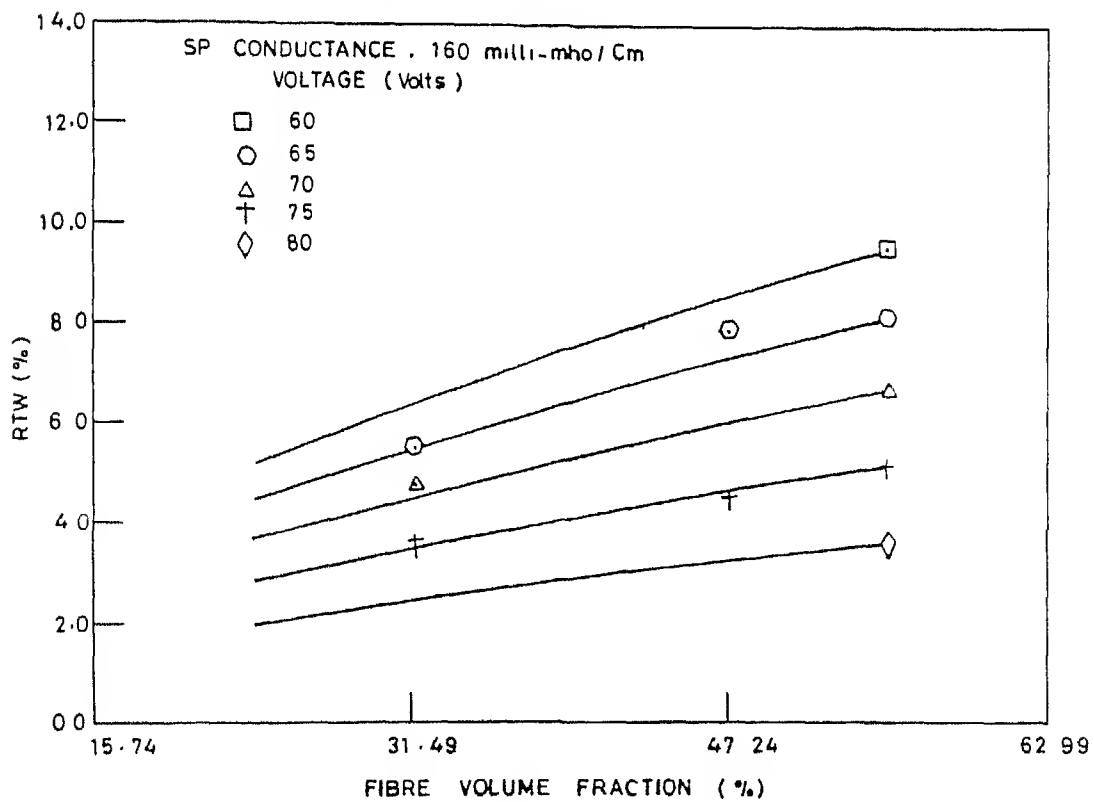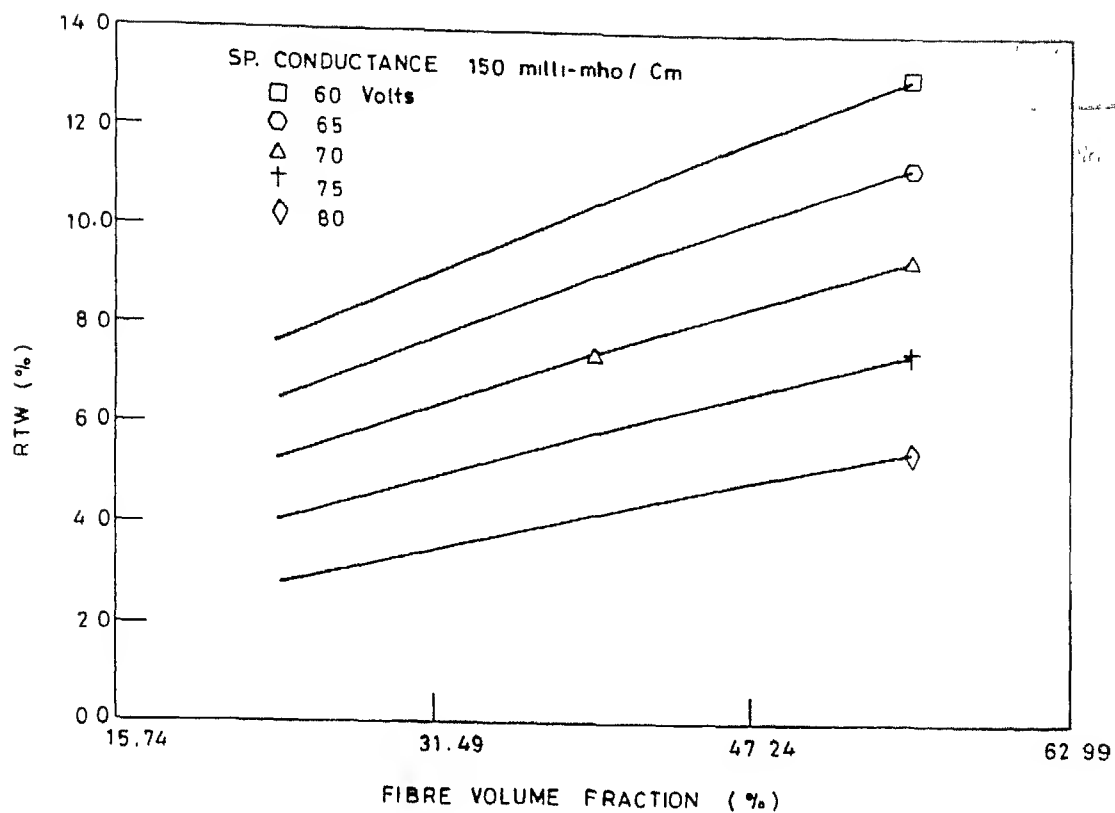
FIG. 3.8 EFFECT OF SP. CONDUCTANCE ON RTW
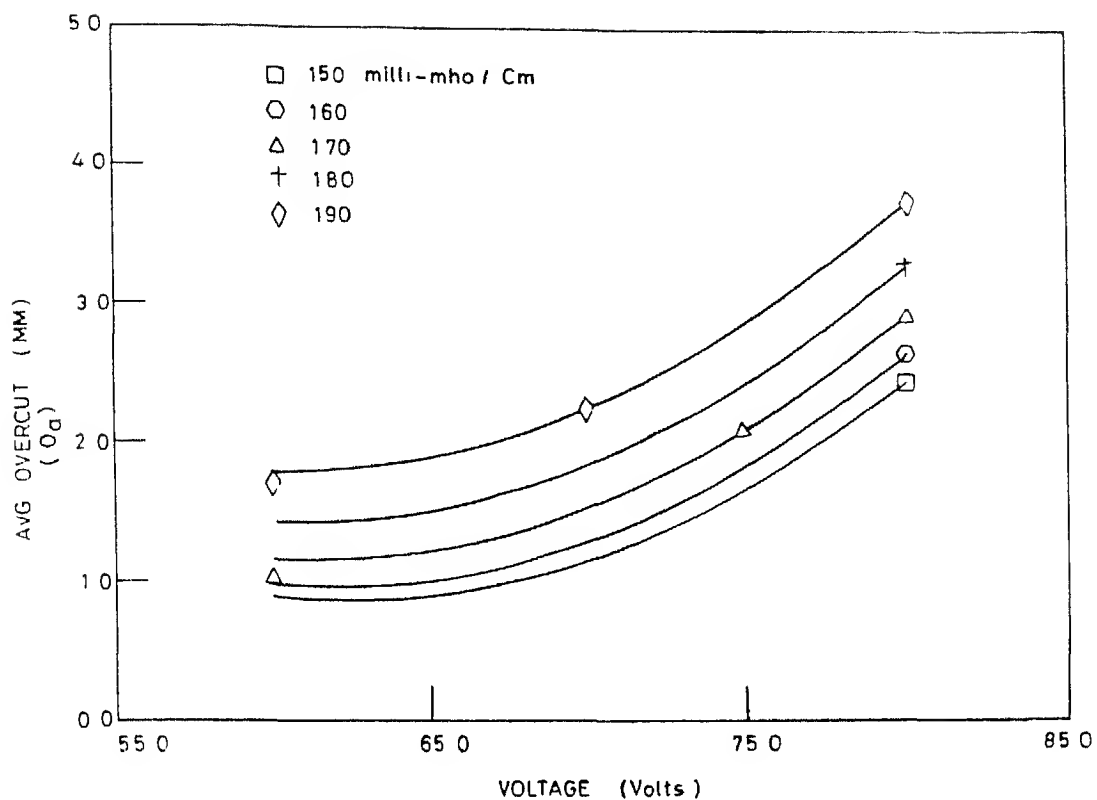
FIG. 3.9 EFFECT OF FIBRE VOLUME FRACTION ON RTW
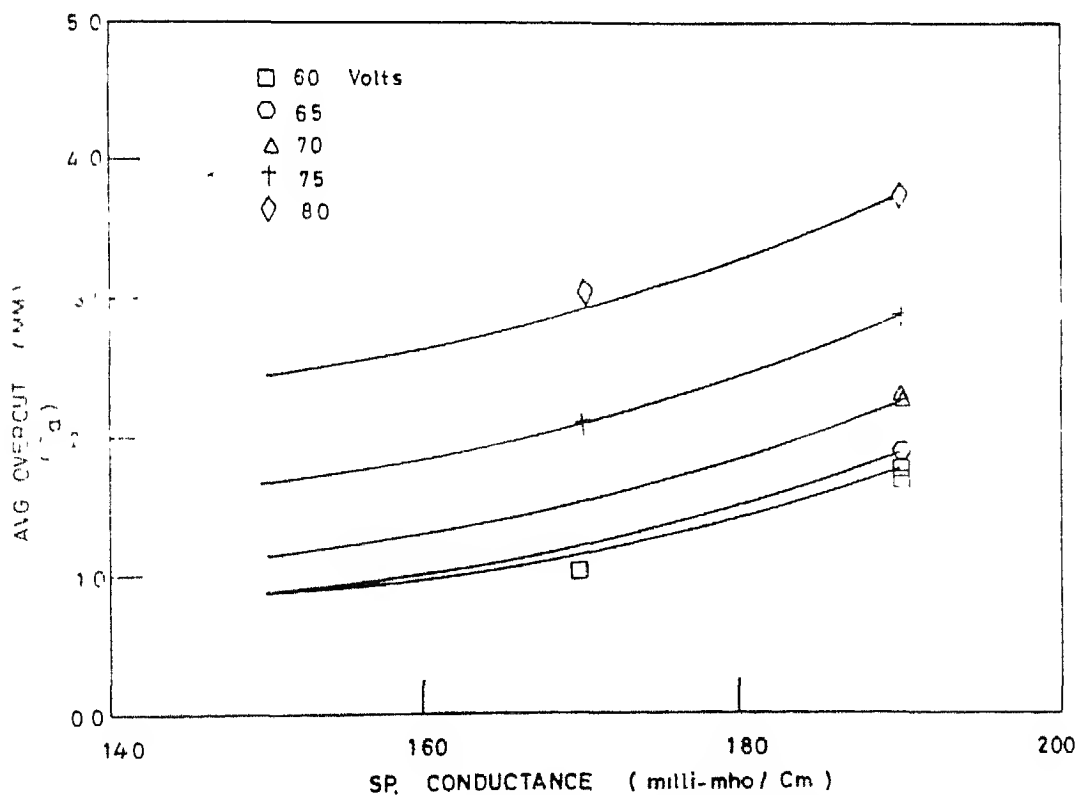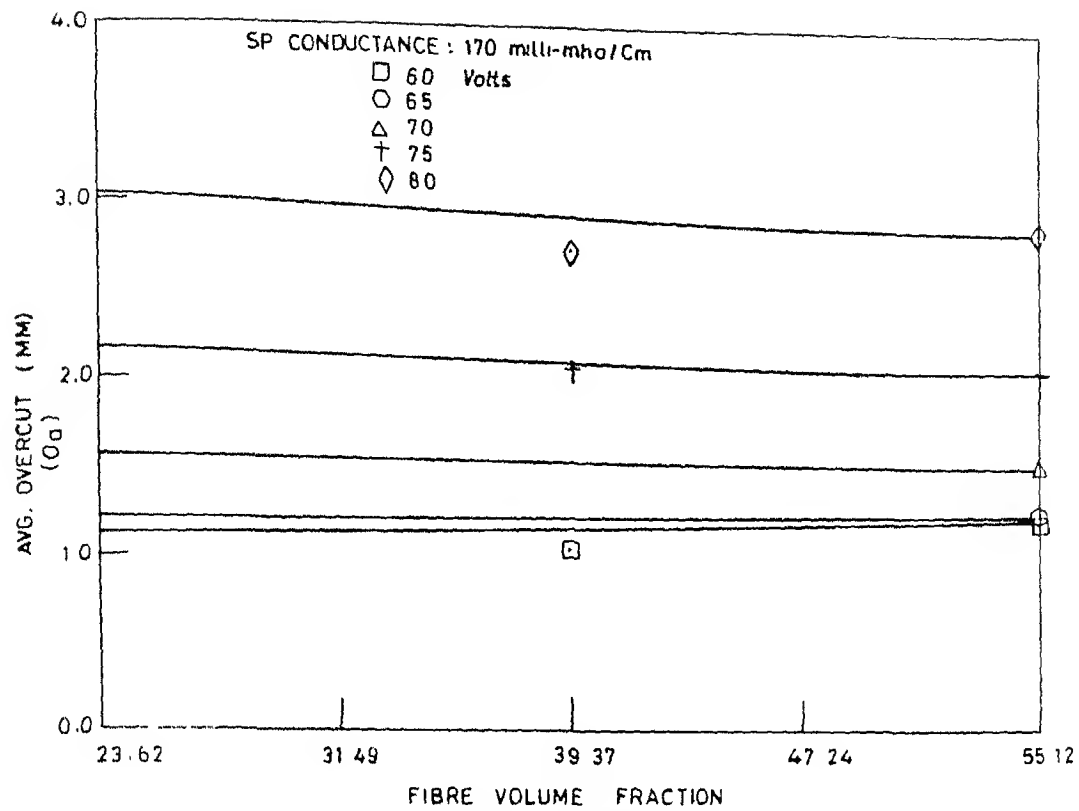
FIG. 3.10 EFFECT OF VOLTAGE ON AVG. OVERCUT

FIG. 3.11 EFFECT OF SP. CONDUCTANCE ON
AVG. OVERCUT
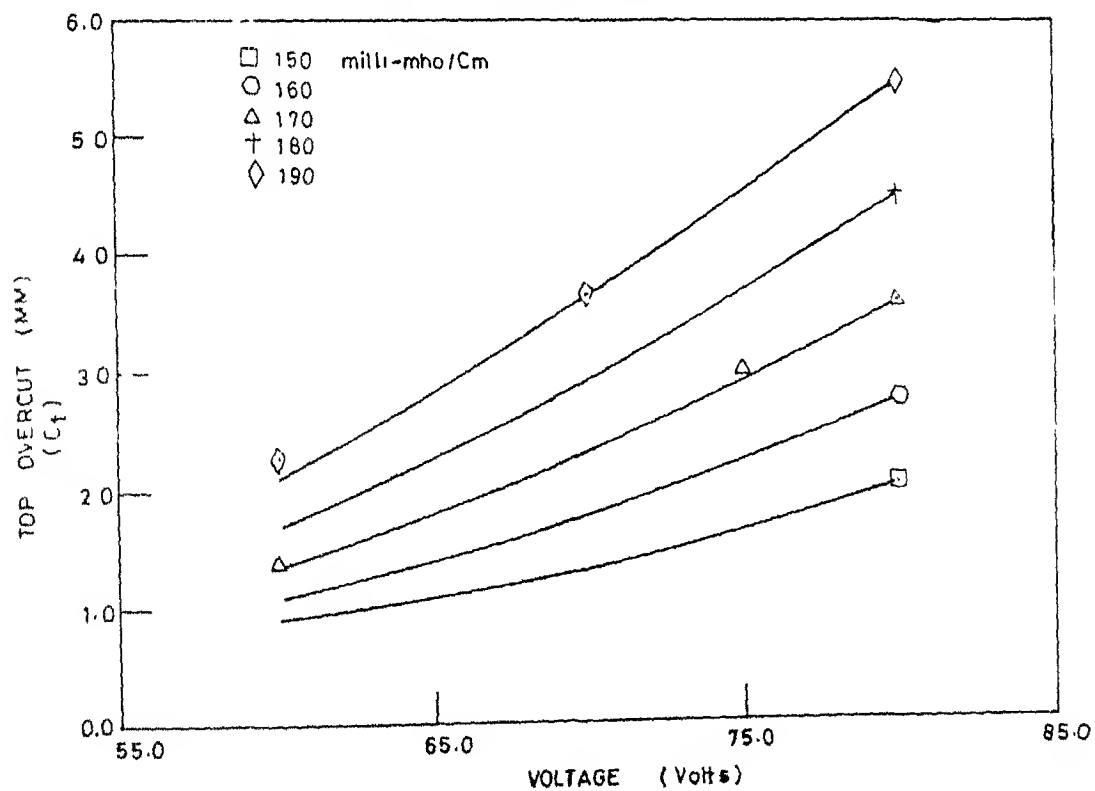
FIG.3.12 EFFECT OF FIBRE VOLUME FRACTION
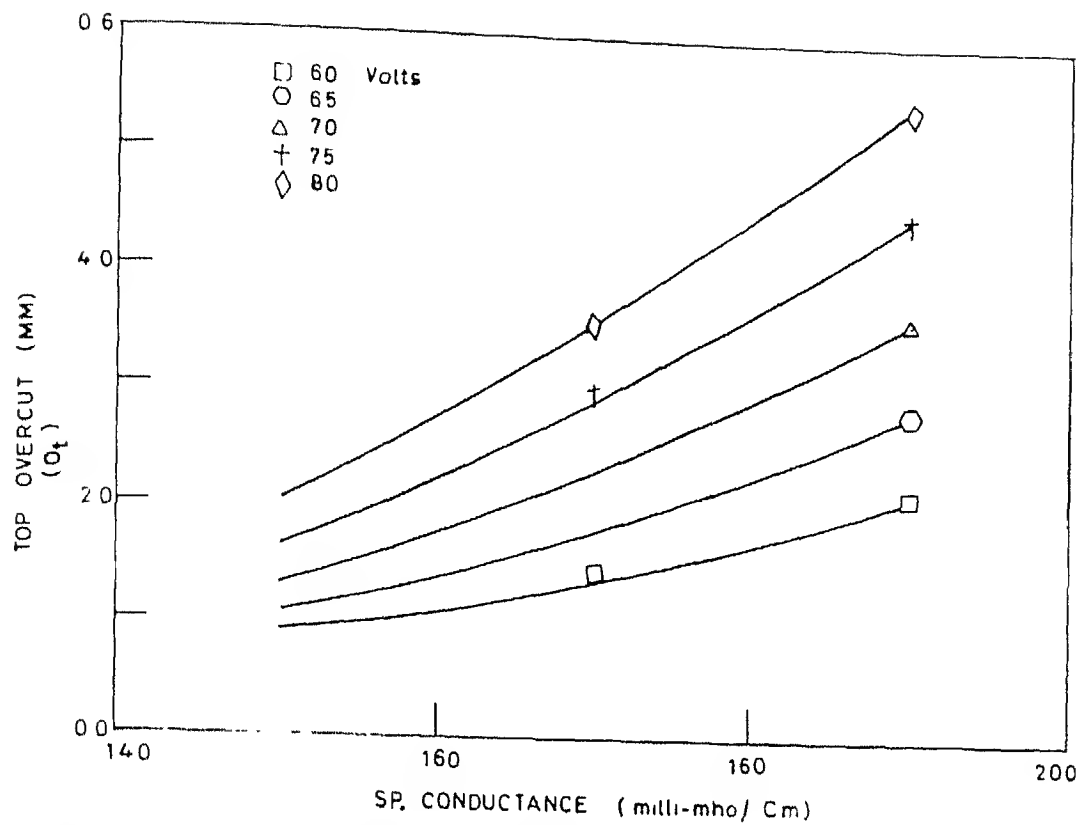ON AVG. OVERCUT

FIG.3.13 EFFECT OF VOLTAGE ON TOP OVERCUT
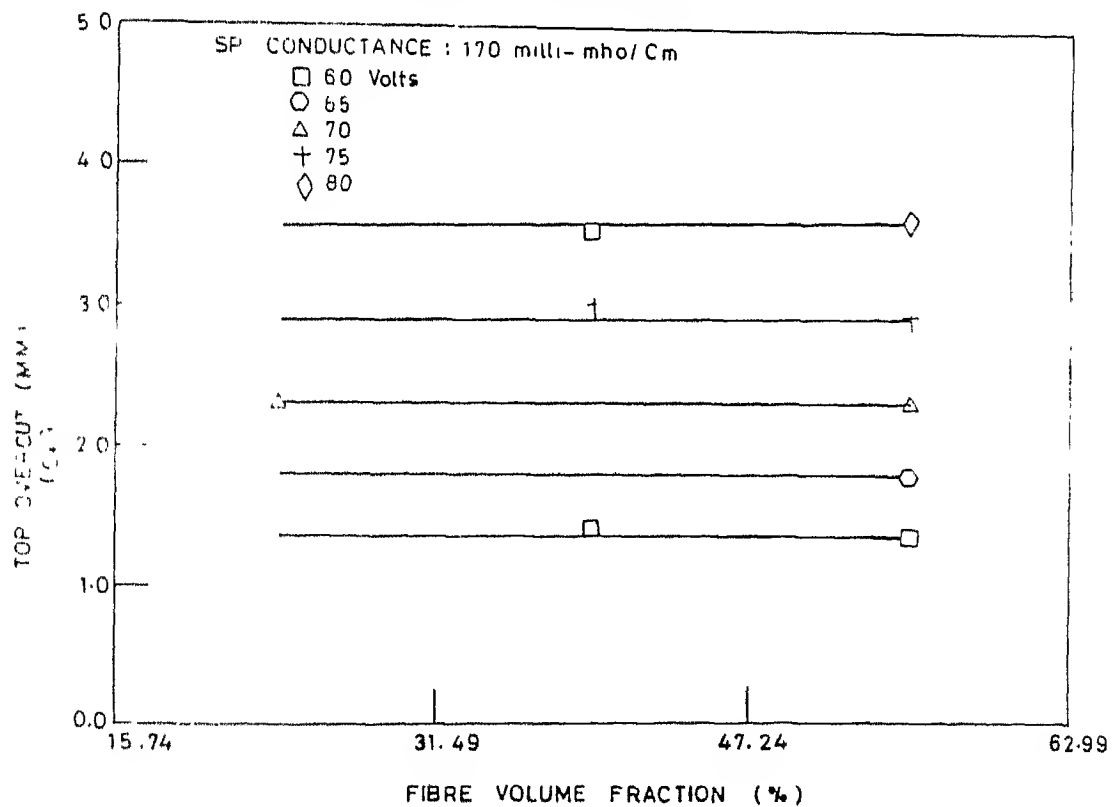
FIG. 3.14   EFFECT OF SP. CONDUCTANCE ON TOP OVERCUT

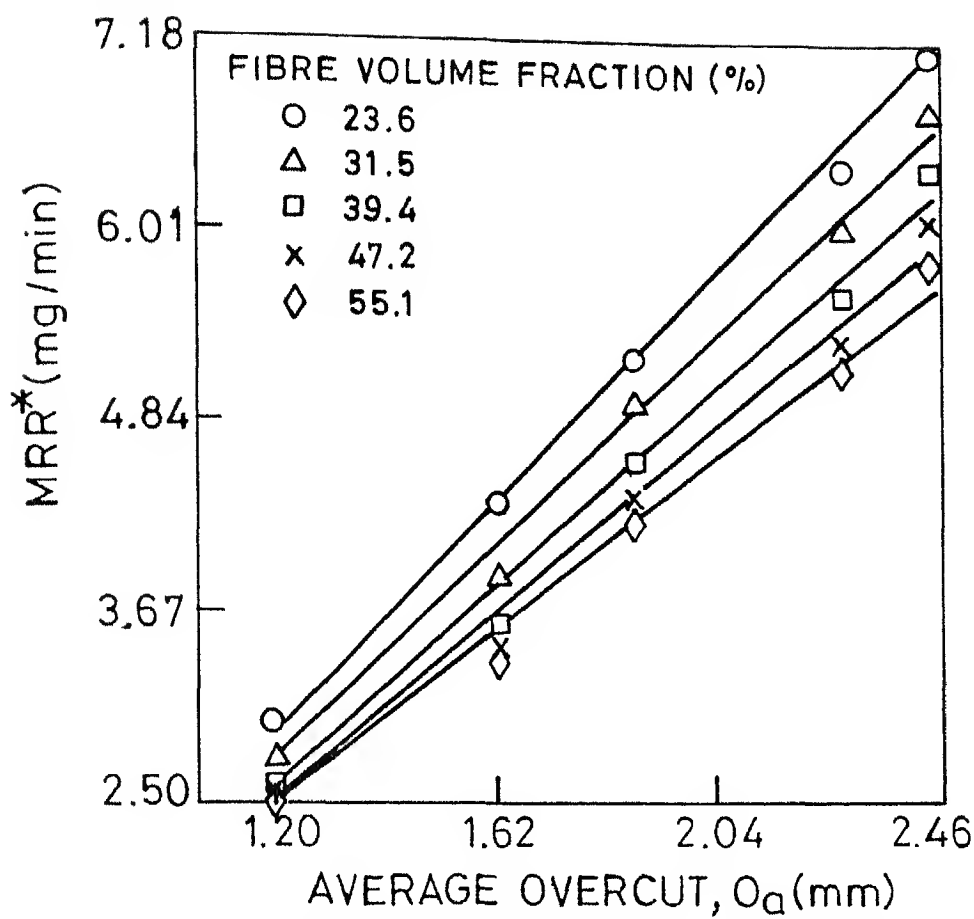FIG. 3.15   EFFECT OF FIBRE VOLUME FRACTION ON TOP OVERCUT
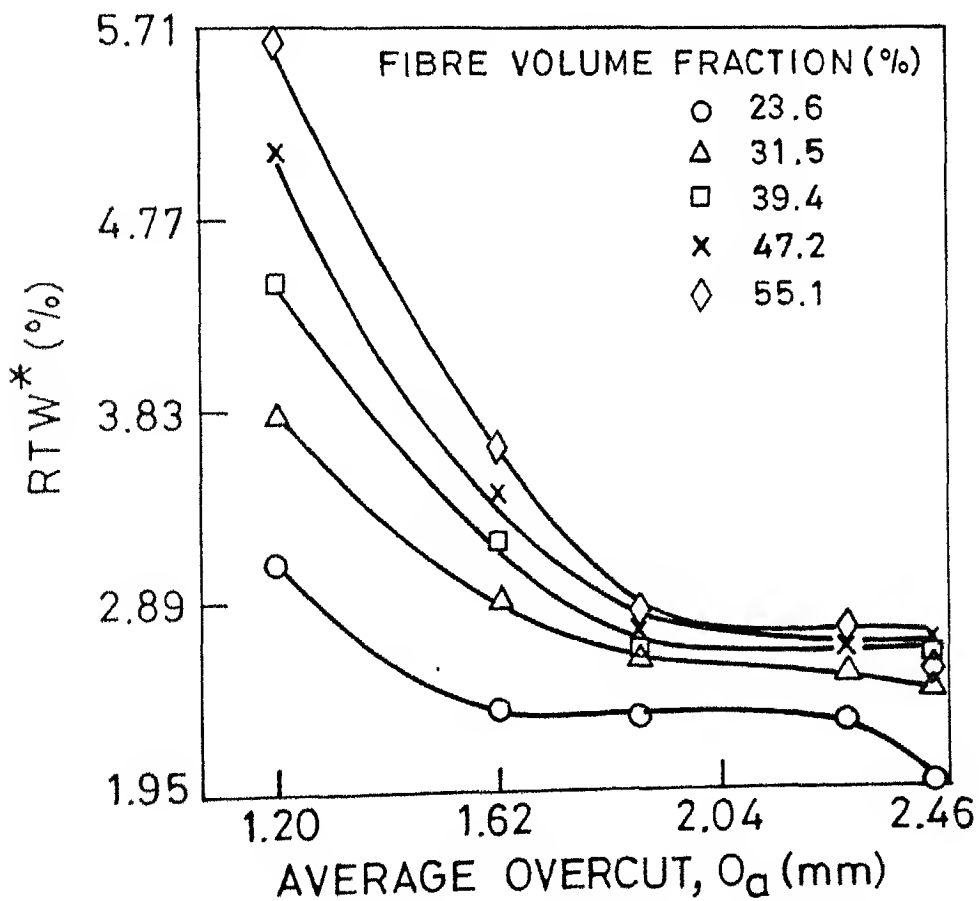
FIG.3.16 EFFECT OF AVERAGE OVERCUT ON MRR*

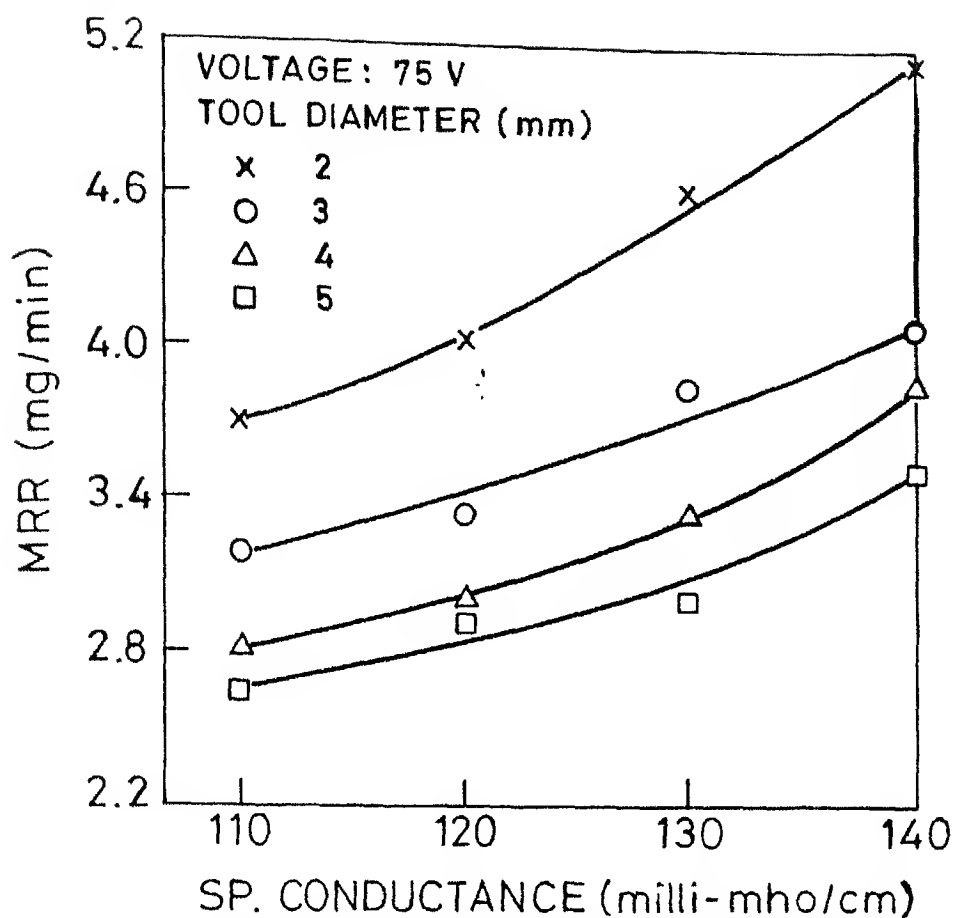FIG.3.17 EFFECT OF AVERAGE OVERCUT ON RTW.*

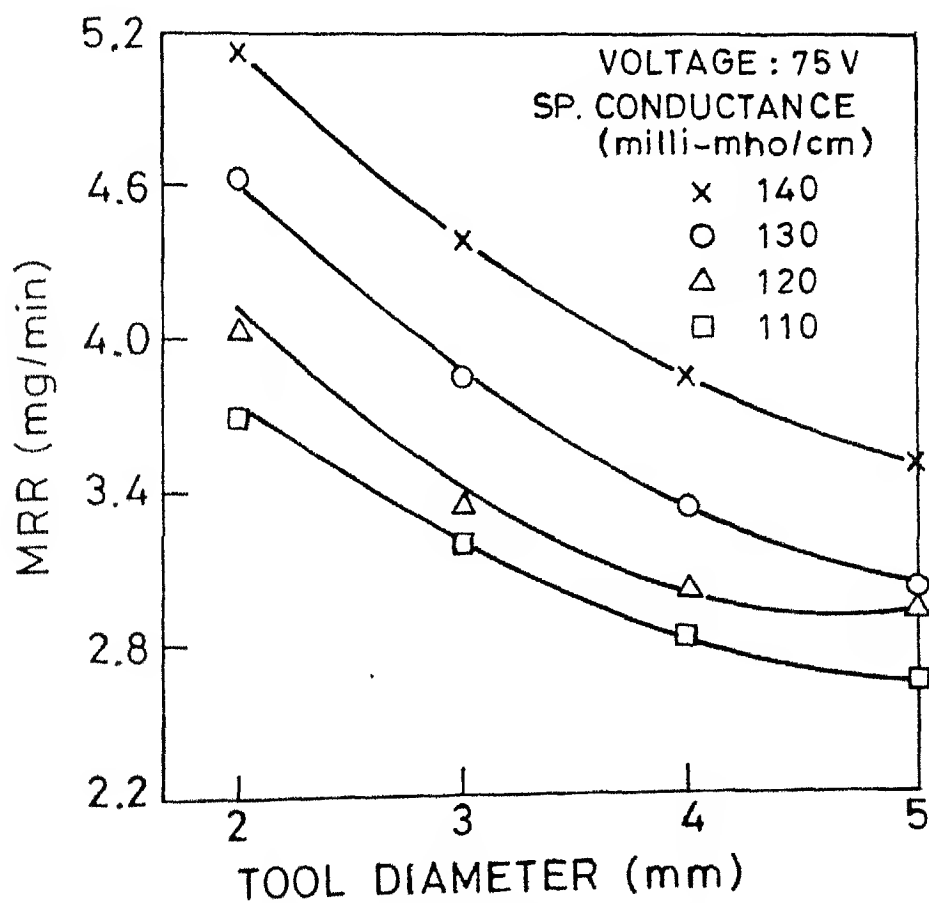FIG. 3.18 EFFECT OF SP. CONDUCTANCE ON MRR.
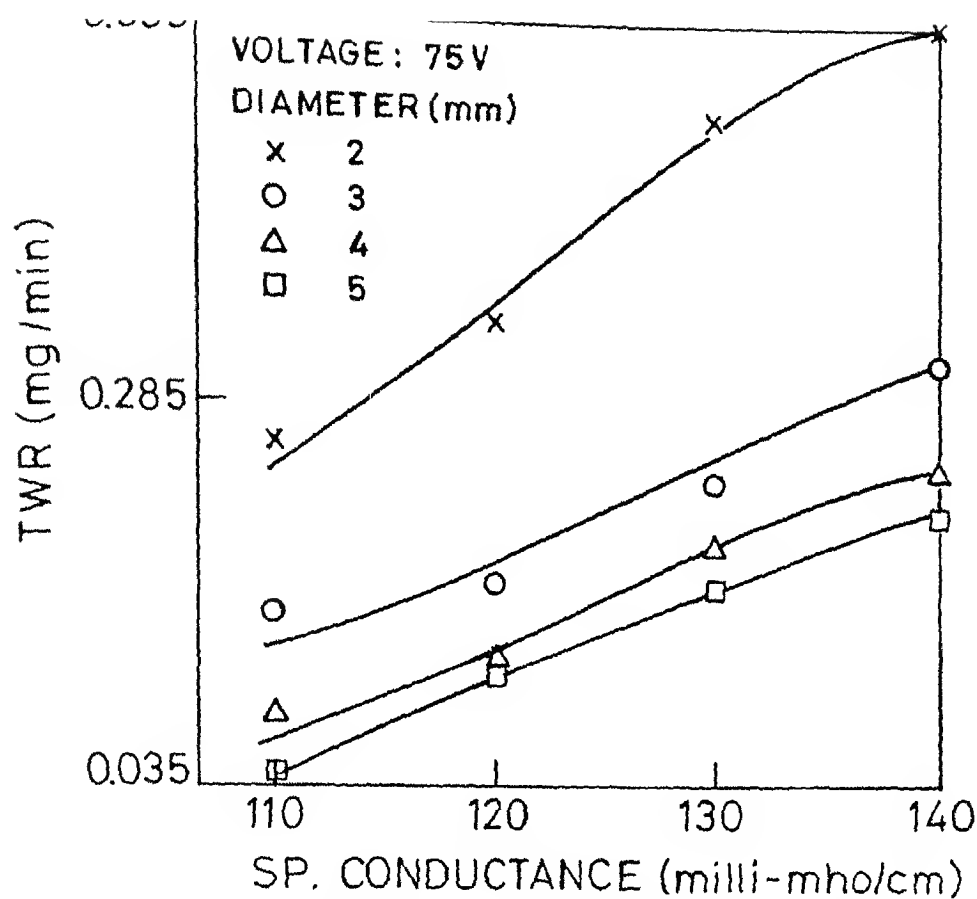

FIG. 3.19 EFFECT OF TOOL DIAMETER ON MRR.

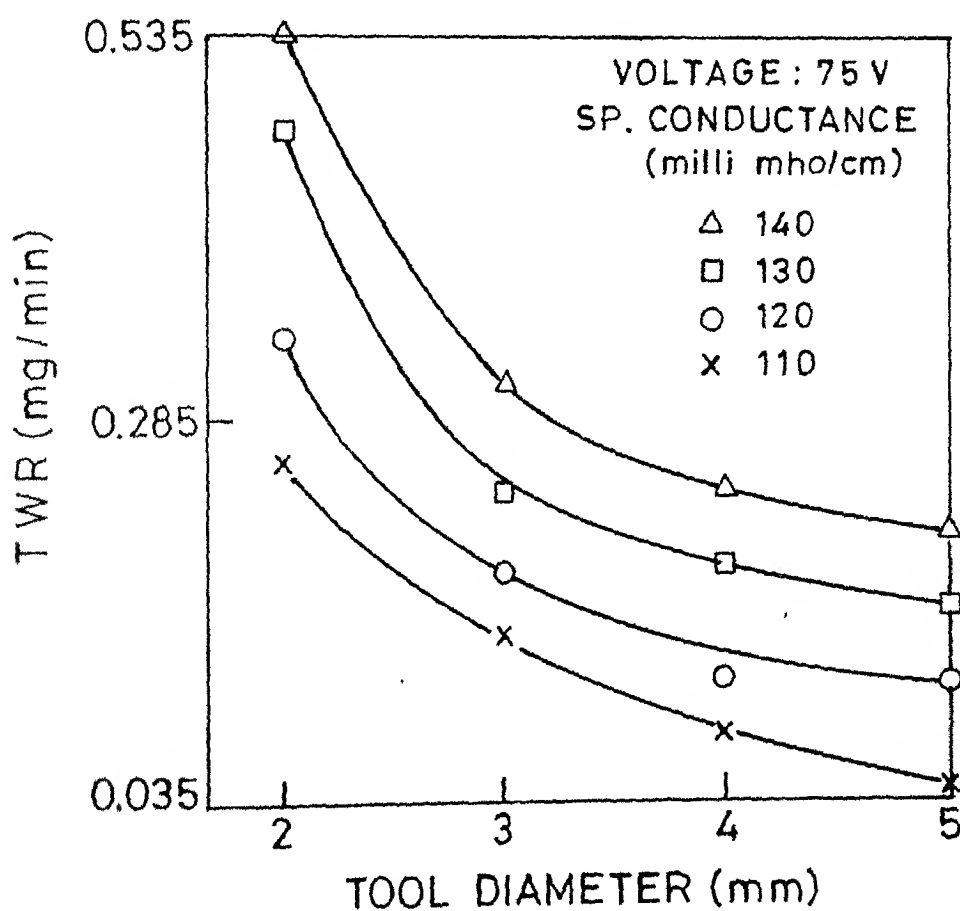FIG. 3.20 EFFECT OF SP. CONDUCTANCE ON TWR.
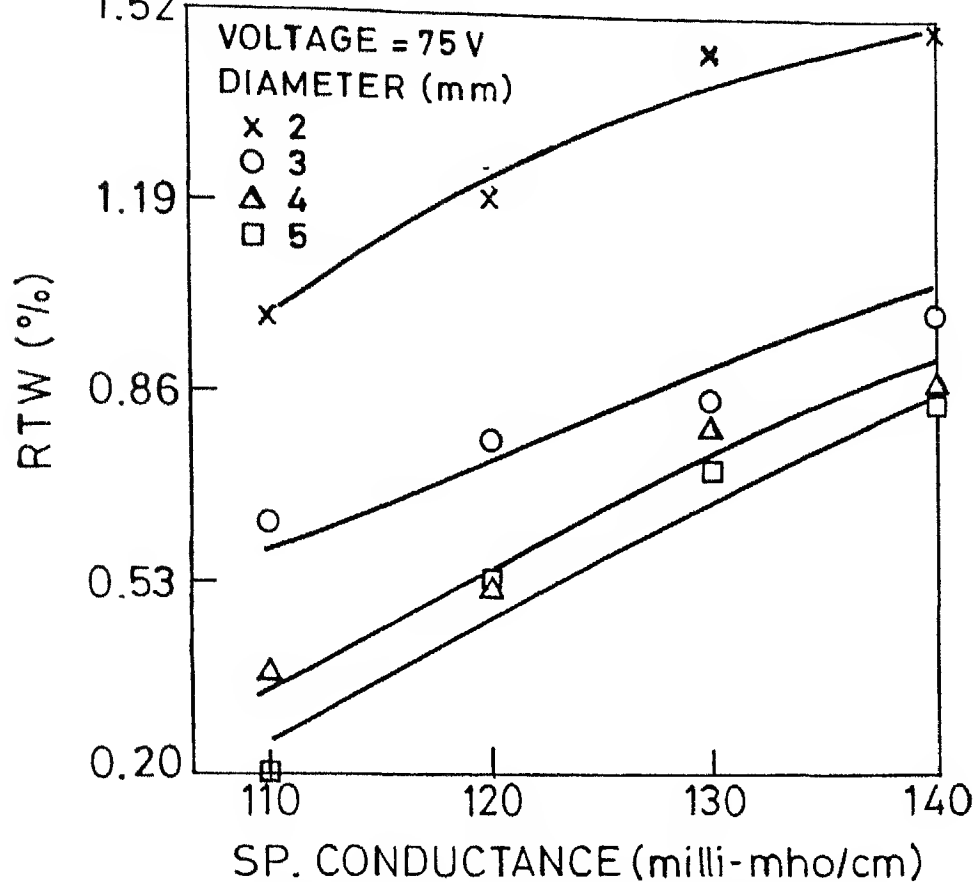

FIG. 3.21 EFFECT OF TOOL DIAMETER ON TWR.

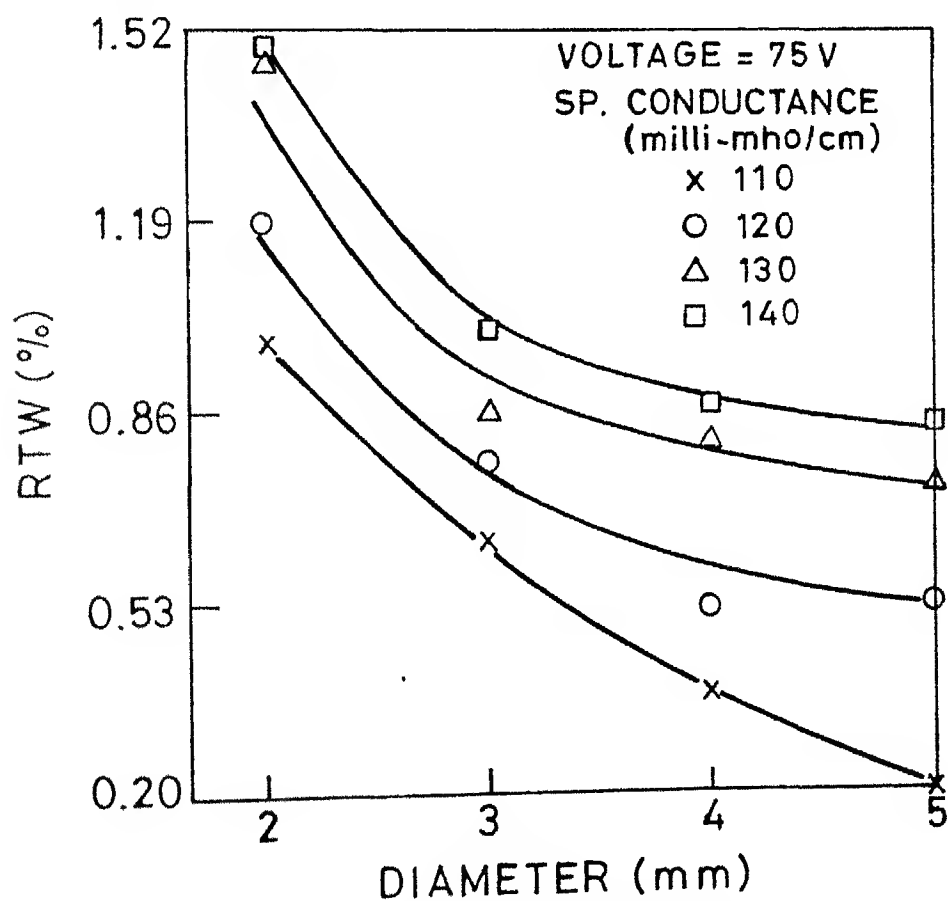FIG. 3.22 EFFECT OF SP. CONDUCTANCE ON RTW
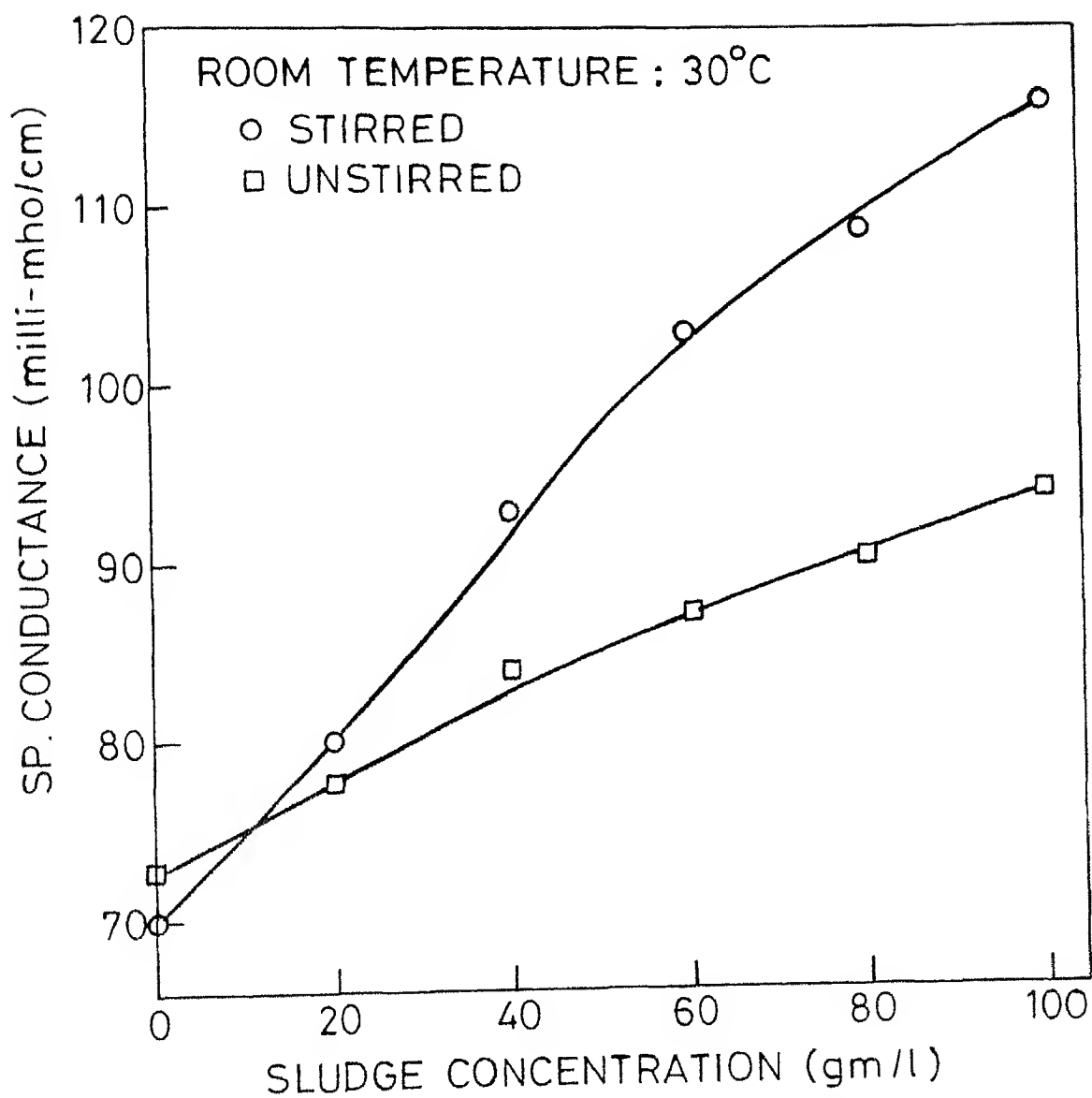

FIG. 3.23 EFFECT OF DIAMETER ON RTW.

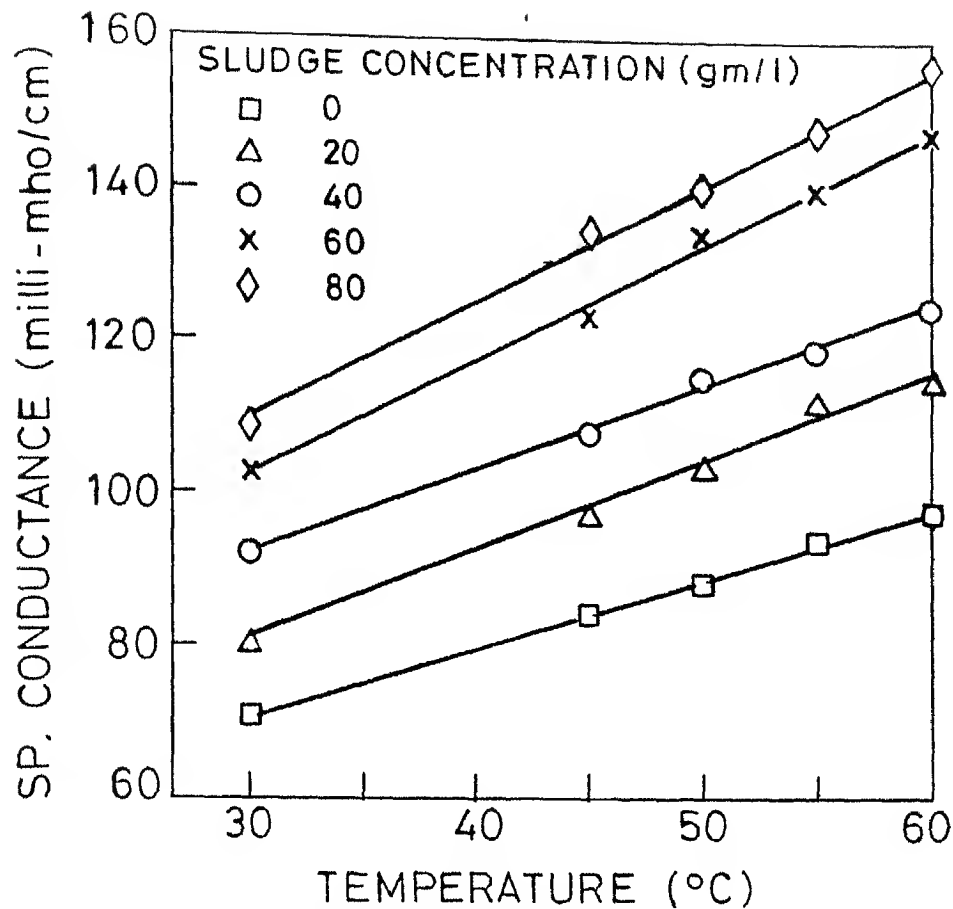FIG. 3.26 EFFECT OF SLUDGE CONCENTRATION ON
SP. CONDUCTANCE

FIG. 3.27 EFFECT OF TEMP. ON SP. CONDUCTANCE.
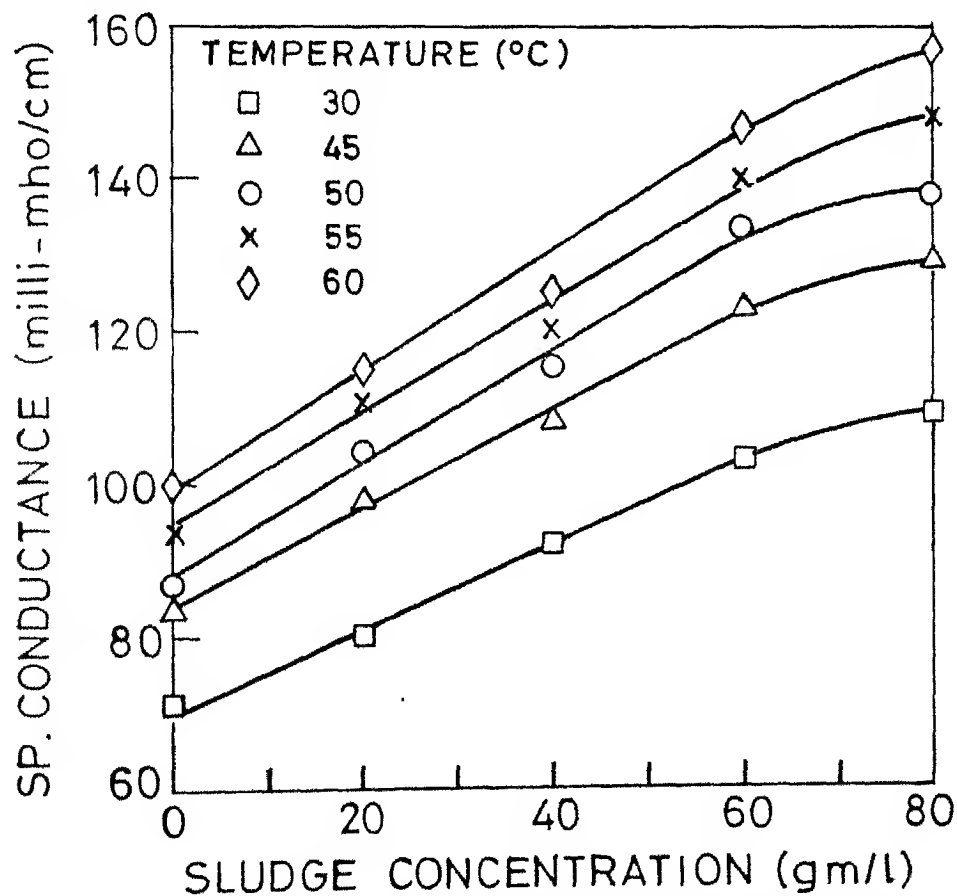
FIG. 3.28 EFFECT OF SLUDGE CONCENTRATION ON SP. CONDUCTANCE.

CHAPTER 4

CONCLUSIONS AND SCOPE FOR FUTURE WORK

4.1 CONCLUSIONS

For the work and tool material used in experimentation at the specified machining conditions, following conclusions have been drawn:

1. Material removal rate increases with increase in voltage or electrolyte conductivity and decreases with fibre volume fraction in the case of glass-epoxy composite cutting. It also decreases with increasing tool diameter.

2. Tool wear rate is found to increase with increasing voltage as well as electrolyte conductivity while it decreases with increasing diameter of tool.Fibre volume fraction has no effect on tool wear rate.

3. In the case of glass-epoxy composite cutting, relative tool wear is observed to decrease with increase in voltage or electrolyte conductivity and it increases with rise in fibre volume fraction. In Kevlar-epoxy composite machining, relative tool wear increases with electrolyte conductivity and decreases with increase in tool diameter.

4. Overcut produced increases with rise in either voltage or electrolyte conductivity and decreases

with increase in tool cross-section. It is
unaffected by a change in fibre volume fraction
in the case of glass-epoxy cutting.

5(i)   Highest achievable material removal rate (MRR*),
in the case of glass-epoxy composite, for a given
overcut, increases linearly with overcut.

(ii)   For glass-epoxy composite machining, minimum relative
tool wear (RTW*) that can be attained at a given
overcut decreases with increase in overcut. The
decrease is quite steep upto an overcut of 1.88 mm
after which there is not much change in RTW*.

(iii) For a given overcut the optimum operating conditions
corresponding to MRR* are independent of fibre volume
fraction.

6.   Specific conductance of the electrolyte increases
linearly with change in temperature.

7.   Specific conductance of the electrolyte increases
with increase in sludge concentration and the relation-
ship is non-linear.

4.2 SCOPE FOR FUTURE WORK

1.   Effect of different electrolytes and their combinations
on MRR, TWR and overcut can be studied.

2.   A theoretical model can be developed for the mechanism
of the process.

3.   Heating of tool through an external source can be
      tried since it will allow more hydrogen to be
      generated near the surface and thus improve MRR.

4.   Pulsed D.C. can also be tried to see the effect on
      MRR and surface finish, as it would essentially
      mean a controlled input of energy in small units.

REFERENCES

1. Konig W., Machining of Fibre reinforced plastics, Annals of CIRP, Vol. 34, 1985, pp. 537-548.

2. Radhakrishnan T. and Wu S.M., On line hole quality evaluation for drilling composite materials using dynamic data, Journal of Engineering for Industry, Vol. 103, 1981, pp. 119-125.

3. Cook N.H., Foot G.B., Jordan P. and Kalyani B.N., Experimental Studies in Electro-machining, Journal of Engineering for Industry, Nov. 1973, pp. 945-950.

4. Schwartz M.M., Composite material handbook, McGraw-Hill Book Company, 1984, Chapter 6.

5. Konig W., New developments in drilling contouring of composites containing Kevlar, SAMPE fifth technology conference, Vol. 2, June 1984, paper 16.

6. Engemann B.K., Water Jet Cutting of Fibre Reinforced Composite Materials, Industrial and Production Engineering, Vol. 3., 1981.

7. Kumar N.U., An Experimental Study of Electrical Machining of non-conducting Materials, M. Tech. Thesis, IIT Kanpur, March, 1985.

8. Larsson C.N. and Baxter E.M., Tool Damage by Sparking in ECM, IMTDR, 1977, p. 499.

9. Loutrel S.P. and Cook N.H., High Rate Electrochemical Machining, Journal of Engineering for Industry, Nov. 1973 pp. 992-996.

10. Khayry A.B.M. and Mc Geough J.A., Modelling of Electro-chemical Arc Machining by Use of Dynamic Data Systems.

11. Mc Geough, J.A. and Crichton I.M., Studies of the Dischar Mechanisms in Electrochemical Arc Machining, Journal of Applied Electrochemistry, Vol. 15, 1985, pp. 113-119.

12. Aggarwal B.D. and Broutman L.J., Analysis and Performance of Fibre Composites, Wiley Interscience Publication, 1980.

13. Cochrain G.W. and Cox M.G., Experimental Designs, Asia Publishing House, 1977.

14.   Adler Yo P., Markova E.V. and Granousky Yu V.,
        The Design of Experiments to Find Optimal Conditions,
        Mir Publishers, Moscow, 1975.

15.   Kothandaraman C.P. and Subramanyam S., Heat and Mass
        Transfer Data Book, Wiley Eastern Limited, 1983.

16.   Jain V.K. and Pandey P.C., Computer Aided Analysis
        of ECBD Process, Proc. of the 23rd IMTDR Conference,
        1982, pp. 257-264.

17.   Bhattacharya A., New Technology, The Institution of
        Engineers (India), 1982.

18.   Barrow G.M., Physical Chemistry, Mc-Graw Hill Book
        Company, 1966.

APPENDIX A

In this appendix results of glass-epoxy composite cutting are tabulated. The experiments were performed according to "design of experiments" concept. Different combinations of the independent parameters, i.e. voltage, specific conductance of electrolyte and fibre volume fraction, and the responses obtained at each such combination are recorded in Table A-1. Five additional experiments were performed to check the validity of the models obtained from the above mentioned responses. The results of these experiments are presented in Table A-2.

TABLE A-1

Glass-epoxy Composite Cutting

Sl. No.	Voltage (volts)	Fibre volume fraction (%)	Sp.conductance (milli-mho/cm)	MRR (mg/min)	TWR (mg/min)	RTW (%)	Average overcut (mm) O_a	Top overcut (mm) O_t
1	65	31.5	160	1.863	0.555	5.416	1.07	1.36
2	75	31.5	160	3.557	0.707	3.616	1.84	2.26
3	65	47.2	160	1.570	0.591	7.730	1.11	1.39
4	75	47.2	160	2.991	0.654	4.497	1.79	2.21
5	65	31.5	180	3.743	0.635	3.084	1.57	2.28
6	75	31.5	180	6.674	0.805	2.195	2.42	3.64
7	65	47.2	180	3.553	0.614	3.554	1.59	2.22
8	75	47.2	180	5.956	0.789	2.726	2.39	3.69
9	60	39.4	170	2.153	0.544	4.869	1.02	1.38
10	80	39.4	170	7.212	0.891	2.379	3.01	3.58
11	70	23.6	170	4.053	0.659	2.771	1.56	2.31
12	70	55.1	170	3.255	0.669	4.447	1.48	2.35
13	70	39.4	150	1.487	0.565	7.324	1.12	1.32

1	2	3	4	5	6	7	8	9
14	70	39.4	190	5.153	0.741	2.772	2.24	3.64
15	70	39.4	170	3.493	0.675	3.722	1.52	2.32
16	70	39.4	170	3.344	0.708	4.079	1.58	2.41
17	70	39.4	170	3.215	0.643	3.851	1.62	2.38
18	70	39.4	170	3.737	0.680	3.509	1.46	2.24
19	70	39.4	170	3.827	0.721	3.631	1.54	2.27
20	70	39.4	170	3.233	0.628	3.743	1.39	2.29

TABLE A-2

Additional Experiments

1	2	3	4	5	6	7	8	9
1	60	47.2	180	2.829	0.574	4.173	1.34	1.72
2	60	39.1	190	3.201	0.579	3.483	1.70	2.28
3	70	23.6	180	5.002	0.712	2.427	1.88	2.92
4	70	31.5	160	2.415	0.624	4.700	1.31	1.78
5	75	39.4	170	4.905	0.763	2.996	2.06	2.98

APPENDIX B

In this appendix results obtained from the computer
program CADEAG-1 for different response surface models are
presented. The response surface equation (Eq. 3) is repro-
duced below for convenience:

$$Y_u = B_o + \sum_{i=1}^{K} B_i X_i + \sum_{i=1}^{K} B_{ii} X_i^2 + \sum_{i < j} B_{ij} X_i X_j$$

Various notations involved in the above equation have been
defined earlier in Section 2.3.2. Values of the coefficients
B_i's, B_{ii}'s and B_{ij}'s for different responses (MRR, TWR, etc.)
are given in Table B-1. Fratios for linear, higher order and
interactive effects of parameters under investigation, (X_1, X_2
and X_3) are recorded in Table B-2. Significant values are
denoted by a symbol (*).

TABLE B-1

Values of Constants of Response Surface Model
for Different Factors

Sources	MRR	TWR	RTW	O_a	O_t
B_o	3.466	0.674	3.773	1.525	2.314
B_1	1.160	0.078	-0.733	0.443	0.559
B_2	-0.210	-0.002	0.472	-0.011	0.003
B_3	1.079	0.043	-1.175	0.275	0.578
B_{11}	0.298	0.009	-0.024	0.128	0.038
B_{22}	0.041	-0.004	-0.028	0.004	0.001
B_{33}	-0.043	-0.006	0.332	0.044	0.039
B_{12}	-0.100	-0.010	-0.172	-0.018	0.004
B_{13}	0.277	0.016	0.415	0.025	0.139
B_{23}	-0.006	-0.002	-0.274	0.000	0.001

O_a — Average overcut

O_t — Top overcut.

TABLE B-2

Fratios for Different Factors

Sources	MRR	TWR	RTW	O_a	O_t
X_1	181.58^*	90.647^*	45.92^*	330.13^*	2042.07^*
X_2	5.956^*	0.068	19.01^*	0.21	0.06
X_3	157.22^*	27.296^*	118.02^*	127.50^*	2181.27^*
X_1^2	18.80^*	2.140	0.081	43.22^*	15.22^*
X_2^2	0.35	0.33	0.11	0.04	0.01
X_3^2	0.39	0.98	14.76^*	5.12^*	15.22^*
X_1X_2	0.68	0.81	1.26	0.26	0.05
X_1X_3	5.18^*	1.94	7.34^*	0.53	62.82^*
X_2X_3	0.00	0.05	3.21	0.00	0.01

X_1 — Voltage

X_2 — Fibre Volume Fraction

X_3 — Specific Conductance

O_a — Average Overcut

O_t — Top Overcut.

APPENDIX C

Here the results obtained from the graphical optimization of glass-epoxy composite cutting, as discussed in Section 3.2, are tabulated. Table C-1 gives the optimum values of material removal rate (MRR^*) for a given overcut and different fibre volume fractions, alongwith optimum operating conditions. Similarly, the optimum values of relative tool wear (RTW^*) are recorded in Table C-2.

TABLE C-1

Optimum MRR Values

Average overcut (mm)	Fibre Volume Fraction (%)					Optimum operating conditions	
	23.6	31.5	39.4	47.2	55.1	V*	k*
1.20	2.98	2.75	2.60	2.56	2.53	65.00	170
1.62	4.33	3.89	3.58	3.46	3.41	71.12	170
1.88	5.23	4.92	4.61	4.37	4.25	70.38	180
2.26	6.42	6.00	5.61	5.30	5.18	73.75	180
2.44	7.15	6.74	6.40	6.09	5.84	75.12	180

V^* — Optimum voltage in volts

k^* — Optimum specific conductance in milli-mho/cm.

TABLE C-2

Optimum RTW Values

Average overcut (mm)	V_f = 23.6%			V_f = 31.5%			V_f = 39.4%			V_f = 47.2%			V_f = 55.1%		
	V^*	k^*	RTW (%)	V^*	k^*	RTW (%)	V^*	k^*	RTW (%)	V^*	k^*	RTW (%)	V^*	k^*	RTW (%)
1.20	65.00	170	3.08	65.00	170	3.81	65.00	170	4.48	65.00	170	5.09	65.00	170	5.65
1.62	66.88	180	2.38	66.88	180	2.82	66.88	180	3.18	66.88	180	3.42	66.88	180	3.66
1.88	65.00	190	2.32	65.00	190	2.60	65.00	190	2.68	65.00	190	2.72	65.00	190	2.76
2.26	76.25	170	2.29	76.25	170	2.52	73.75	180	2.65	73.75	180	2.70	73.75	180	2.72
2.44	79.00	160	1.97	77.50	170	2.44	75.12	180	2.63	75.12	180	2.68	75.12	180	2.54

V^* — Optimum voltage in volts

k^* — Optimum specific conductance in milli-mho/cm

V_f — Fibre volume fraction (%).

APPENDIX D

In this appendix results of Kevlar-epoxy composite machining are presented. Experiments were carried out at a constant voltage of 75 volts. Copper tools of 2,3,4 and 5 mm diameters were used. For a given tool diameter specific conductance of electrolyte was varied from 110 to 140 milli-mho/cm and MRR, TWR, RTW and diametral overcut were measured/calculated for each experiment.

TABLE D-1

Results of Kevlar-epoxy Composite Machining

Tool diameter (mm)	Sp. conductance (milli-mho/cm)	MRR (mg/min)	TWR (mg/min)	RTW (%)	Diametral overcut, ((mm)
2	110	3.70	0.253	0.987	3.16
	120	4.03	0.333	1.194	3.48
	130	4.63	0.469	1.463	4.07
	140	5.14	0.533	1.498	4.41
3	110	3.19	0.141	0.638	2.06
	120	3.34	0.180	0.779	2.44
	130	3.85	0.227	0.851	2.87
	140	4.39	0.305	1.003	3.82
4	110	2.83	0.073	0.373	1.62
	120	3.01	0.109	0.524	2.01
	130	3.34	0.187	0.809	2.58
	140	3.85	0.233	0.874	3.02
5	110	2.65	0.037	0.202	0.91
	120	2.92	0.107	0.530	1.33
	130	3.01	0.157	0.733	1.91
	140	3.52	0.207	0.850	2.44

APPENDIX E

Experimental results for effect of sludge on specific
conductance of electrolyte are recorded in this appendix.
In Tables E-1 and E-2 values of specific conductance at
different values of sludge concentration, for "stirred"
and "unstirred" conditions, are given. These experiments were
conducted at room temperature. Table E-3 gives the specific
conductance values for different combinations of temperature
and sludge concentration.

TABLE E–1

Effect of Sludge Concentration on Specific
Conductance for "Stirred" Conditions

S.No.	Wt. of sludge (gms.)	Sp. conductance (milli-mho/cm)
1	0	70
2	10	80
3	20	93
4	30	103
5	40	109
6	50	116

TABLE E–2

Effect of Sludge Concentration on Specific
Conductance for "Unstirred" Conditions

S.No.	Wt. of sludge (gms.)	Sp. conductance (milli-mho/cm)
1	0	73
2	10	78
3	20	84
4	30	87
5	40	90
6	50	94

Room temperature : 30°C

Volume of electrolyte: 500 ml.

TABLE E-3

Variation of Specific Conductance with Temperature and
Sludge Concentration for "Stirred" Conditions

| Temp. (°C)	30	45	50	55	60
Wt. of sludge (gms)					
0	71	84	87	92	100
10	80	98	104	111	116
20	92	108	115	119	126
30	103	124	134	140	148
40	109	130	140	149	157

Volume of electrolyte : 500 ml.

APPENDIX F

Shadowgraphs of the machined profile were taken at a magnification of 20X. These were then used to obtain the overcut produced during ECDM of composites. Some of the shadowgraphs of ECDM of glass-epoxy composites are given in Figure F-1 while in Figure F-2 shadowgraphs of machining of blind holes in Kevlar-epoxy composite are given. Different types of overcuts, as obtained from these shadowgraphs, have been defined earlier in Sections 2.3.1 and 2.4.1.
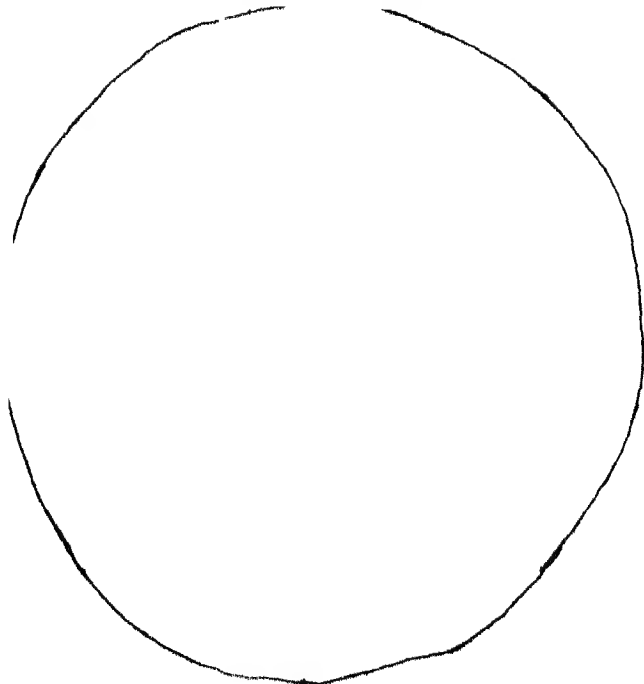
Not to the scale
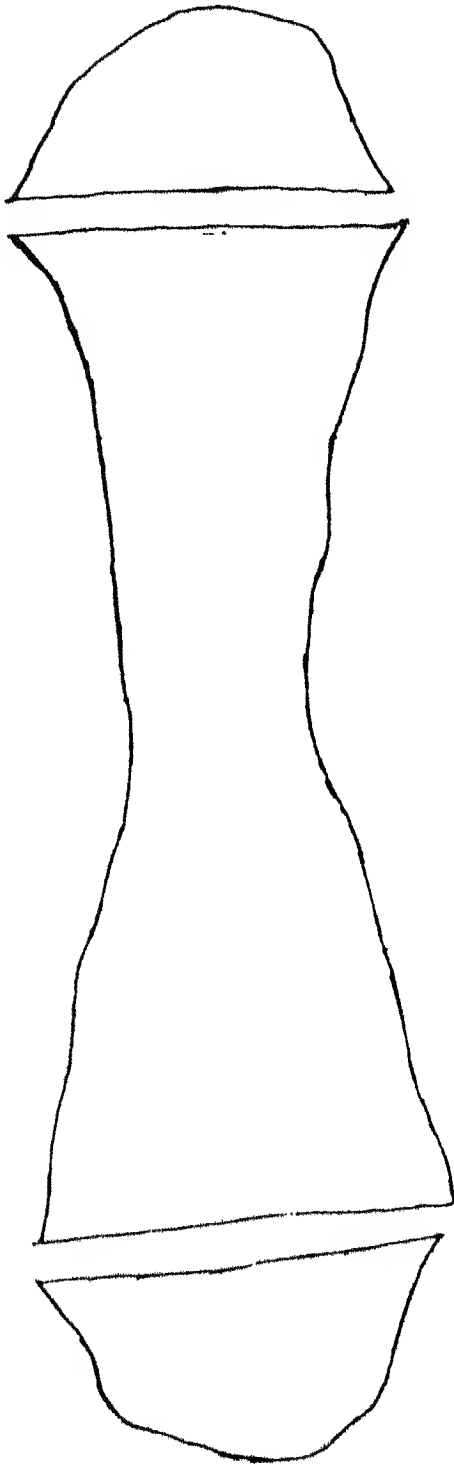
(c)

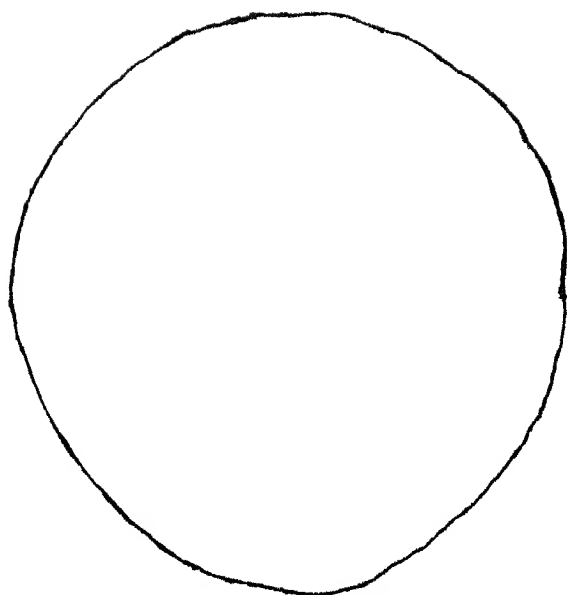S.No.25, TABLE A-1
Tool thickness = 0.57 mm
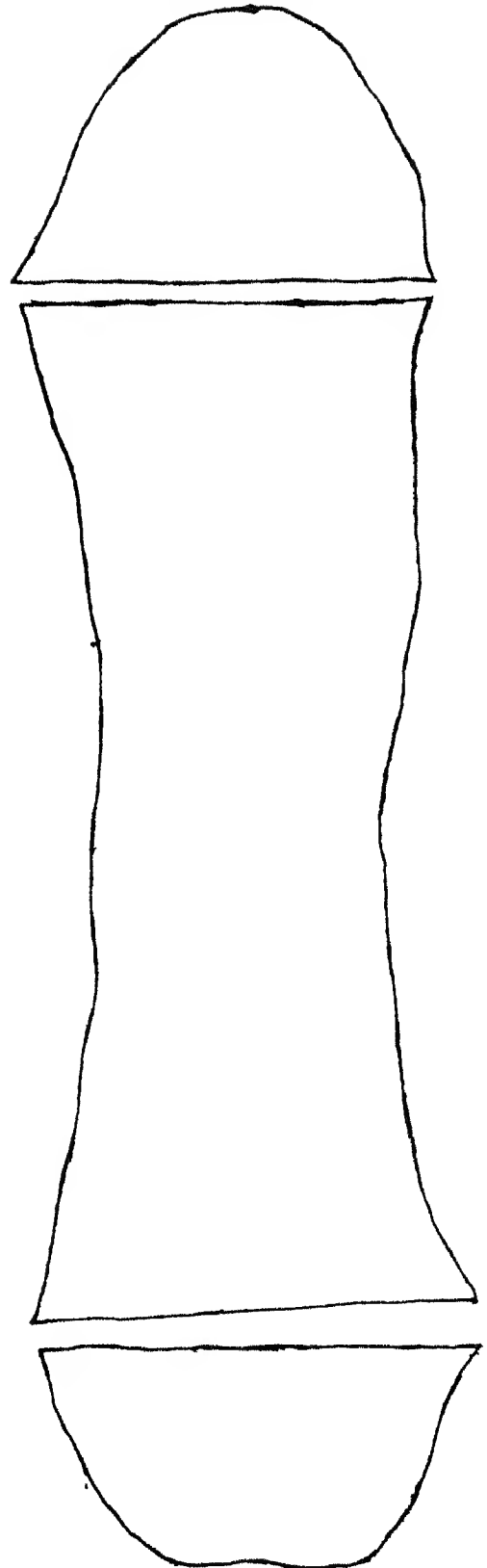
(b)

S.No. 10, TABLE A-1
Tool Thickness = 0.57 mm
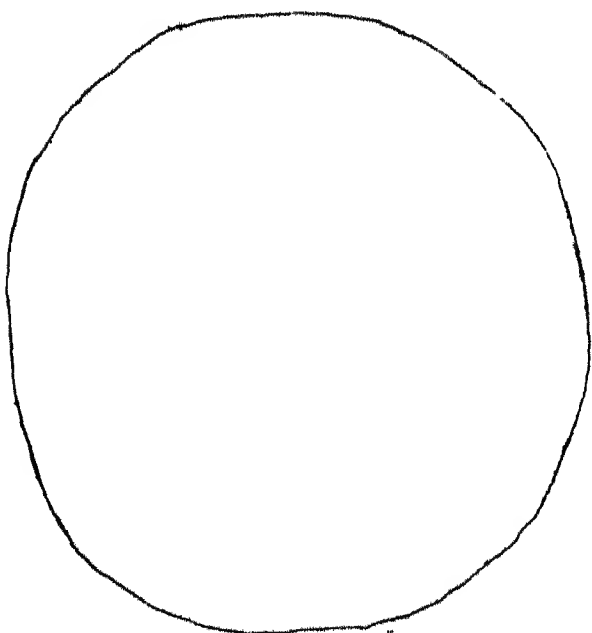
FIGURE F-1 : Shadowgraphs of glass-epoxy composite cutting

(a)

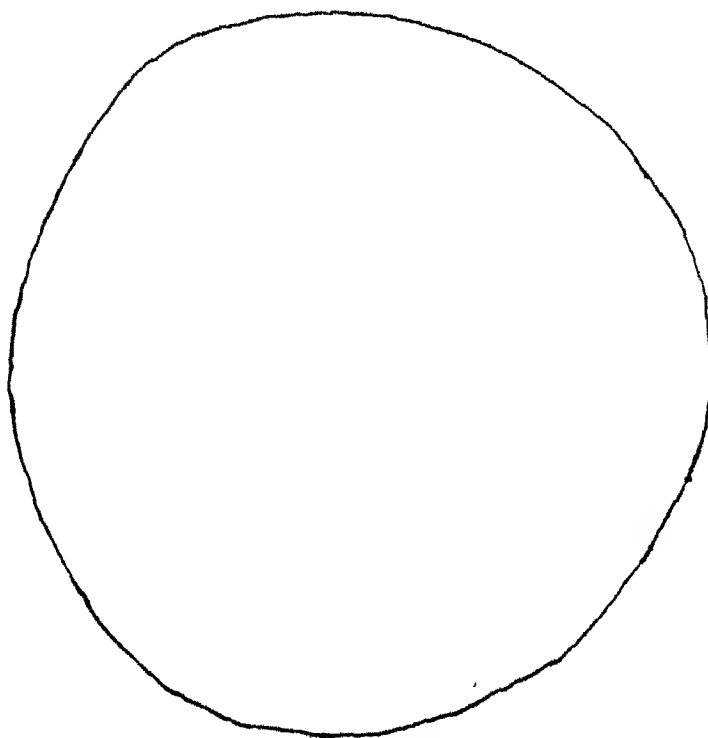Tool diameter = 3.08 mm
Sp. conductance = 130 milli-mho/cm
(Table D-1,

(b)

Tool diameter = 2.04 mm
Sp. conductance = 110 milli-mho/cm
(Table D-1)

(c).

Tool diameter = 4.06 mm
Sp. conductance = 110 milli-mho/cm

(d)

Tool diameter = 4.02 mm
Sp. conductance = 130 milli-mho/cm

FIGURE F-2 :   Shadowgraphs of blind holes in Kevlar-epoxy
composite

ME-1907-M-TAN-MAG